1974

Induced currents on two dimensional electromagnetic planar structures.

Rospigliosi Balta, Jose Alberto; Adler, Richard William

Monterey, California. Naval Postgraduate School

INDUCED CURRENTS ON TWO DIMENSIONAL ELECTROMAGNETIC PLANAR STRUCTURES

José Alberto Rospigliosi Balta

Report Number--NPS52AB74124

NAVAL POSTGRADUATE SCHOOL
Monterey, California

THESIS

INDUCED CURRENTS ON TWO DIMENSIONAL ELECTROMAGNETIC PLANAR STRUCTURES

José Alberto Rospigliosi Balta

December 1974

Thesis Advisor: R. W. Adler

Approved for public release; distribution unlimited.

Prepared for:
Air Force Weapons Lab.
Kirtland AFB, New Mexico 87117

NAVAL POSTGRADUATE SCHOOL
Monterey, California

Rear Admiral Isham Linder
Superintendent

Jack R. Borsting
Provost

This thesis prepared in conjunction with research supported in part by Air Force Weapons Lab under Project Number 75-002, 13 May 74.

Release as a
Technical Report by:

UNCLASSIFIED

SECURITY CLASSIFICATION OF THIS PAGE (When Data Entered)

REPORT DOCUMENTATION PAGE		READ INSTRUCTIONS BEFORE COMPLETING FORM
1. REPORT NUMBER	2. GOVT ACCESSION NO.	3. RECIPIENT'S CATALOG NUMBER
4. TITLE (and Subtitle) INDUCED CURRENTS ON TWO DIMENSIONAL ELECTROMAGNETIC PLANAR STRUCTURES		5. TYPE OF REPORT & PERIOD COVERED 6. PERFORMING ORG. REPORT NUMBER NPS 52AB74124
7. AUTHOR(s) José Alberto Rospigliosi Balta in conjunction with Richard W. Adler		8. CONTRACT OR GRANT NUMBER(s)
9. PERFORMING ORGANIZATION NAME AND ADDRESS Naval Postgraduate School Monterey, California 93940		10. PROGRAM ELEMENT, PROJECT, TASK AREA & WORK UNIT NUMBERS 75-002
11. CONTROLLING OFFICE NAME AND ADDRESS Air Force Weapons Lab. Kirtland AFB, New Mexico 87117		12. REPORT DATE December 1974 13. NUMBER OF PAGES 109
14. MONITORING AGENCY NAME & ADDRESS(if different from Controlling Office)		15. SECURITY CLASS. (of this report) Unclassified 15a. DECLASSIFICATION/DOWNGRADING SCHEDULE

16. DISTRIBUTION STATEMENT (of this Report)

Approved for public release; distribution unlimited.

17. DISTRIBUTION STATEMENT (of the abstract entered in Block 20, if different from Report)

18. SUPPLEMENTARY NOTES

19. KEY WORDS (Continue on reverse side if necessary and identify by block number)

Electromagnetic Pulse (EMP)
Induced Currents
Two-dimensional Structures
Two-dimensional Cross

20. ABSTRACT (Continue on reverse side if necessary and identify by block number)

Electromagnetic pulse has become a possible threat to nearly all sophisticated military systems. The crossed dipole receiving antenna has been used as a representative model to approximate electromagnetic pulse effects on aircraft. A very basic way to approximate an aircraft structure is by a two-dimensional cross.

DD FORM 1 JAN 73 1473 EDITION OF 1 NOV 65 IS OBSOLETE
S/N 0102-014-6601 | 1
(Page 1)

UNCLASSIFIED
SECURITY CLASSIFICATION OF THIS PAGE (When Data Entered)

Block #20 Continued

This paper is an application of the Piecewise-Sinusoidal Reaction Matching Technique (PSRMT) to find the current density distribution in a two-dimensional cross illuminated by a monochromatic plane wave. Other two-dimensional structures are solved previous to the cross structure in order to gain insight and to validate this approach with respect to previous solution techniques.

Induced Currents on Two Dimensional Electromagnetic Planar Structures

by

José Alberto Rospigliosi Balta
Lieutenant, Peruvian Navy
B.S.E.E., Naval Postgraduate School, 1973

Submitted in partial fulfillment of the
requirements for the degree of

MASTER OF SCIENCE IN ELECTRICAL ENGINEERING

from the

NAVAL POSTGRADUATE SCHOOL
December 1974

ABSTRACT

Electromagnetic pulse has become a possible threat to nearly all sophisticated military systems. The crossed dipole receiving antenna has been used as a representative model to approximate electromagnetic pulse effects on aircraft. A very basic way to approximate an aircraft structure is by a two-dimensional cross.

This paper is an application of the Piecewise-Sinusoidal Reaction Matching Technique (PSRMT) to find the current density distribution in a two-dimensional cross illuminated by a monochromatic plane wave. Other two-dimensional structures are solved previous to the cross structure in order to gain insight and to validate this approach with respect to previous solution techniques.

TABLE OF CONTENTS

LIST OF TABLES

LIST OF DRAWINGS

ACKNOWLEDGEMENTS

The author is indebted to a multitude of persons for their assistance and patience during the preparation of this thesis. Foremost, I wish to thank Dr. Richard W. Adler, under whose direct supervision I worked.

I wish to express my thanks to Lt. Kharavuth Khemayodhin for his frequent aid. Thanks is also due to my wife, Alicia, for her confidence and assurance throughout this project.

All computer calculations were conducted at the W. R. Church Computer Center. The cooperation of the Computer Center staff is appreciated.

I. INTRODUCTION

A. NEED FOR STUDY

Electromagnetic pulse has become a possible threat to nearly all sophisticated military systems [Ref. 1]. Under the proper circumstances a significant portion of the energy released during a nuclear detonation will be appear as an Electromagnetic Pulse (EMP) having the same frequencies as those employed by most of our commercial radio and military system equipments.

Any metallic object, such as an aircraft structure, exposed to electromagnetic fields can be a collector of electromagnetic energy, that is, act like an antenna, even though it was never intended to be that.

The crossed-dipole receiving antenna has been used as a representative model to approximate electromagnetic pulse effects on aircraft [Ref. 2]. The crossed-dipole, in this case the aircraft, can be modeled in its simplest way as a two-dimensional structure, that is, a cross with thickness equal to zero.

B. BACKGROUND INFORMATION

Electromagnetic boundary-value problems can be solved exactly via classical separation of variable analysis only for a few geometries, such as the sphere, spheroid, circular cylinder, elliptical cylinder, strip and wedge. Such solutions can be expressed in terms of a summation of a set of eigenfunctions which can be evaluated with a high speed

computer. However, for problems involving complicated geometries the exact solution is not available. Thus, the approximate and numerical methods are of great significance. The research discussed herein is directed toward the numerical solution of the problem of scattering from conducting bodies of arbitrary shape.

Two methods [Ref. 3] are available for electromagnetic modeling of continuous conducting surfaces with arbitrary shape: the wire grid model and the surface current model using rectangular-pulse bases. Both methods have similar limitations with the maximum cell width restricted to approximately $\lambda/10$. Unless the conducting body is symmetric or is a figure of revolution, computer storage requirements have limited the moment-method application to bodies with surface area not exceeding one or two square wavelengths.

In this paper, the piecewise-sinusoidal reaction technique applied by Richmond [Ref. 3] to scattering by conducting bodies of arbitrary shape is used.

C. STATEMENT OF THE PROBLEM

The objective of this research is to find the current distribution in a two-dimensional cross. In order to get an understanding of the "junction problem" that will be present in the cross structure, the induced current density on a perfectly-conducting rectangular plate will be first solved for, this result having been presented by Richmond and Wang [Ref. 3]. Likewise the square plate solved by Rahmat-Samii and Mitra [Ref. 4] will be studied. From this

the complexity of the structure will be increased, solving for current distribution on structures like an L, T and finally the cross.

D. SCOPE AND LIMITATIONS OF THE STUDY

The general solutions steps are:

1) Divide the continuous conducting surface into cells with the surface current distribution being expanded in overlapping sinusoidal bases functions.

2) Via an application of Galerkin's method, the integral equation formulated with the zero-reaction concept is reduced to a matrix equation.

3) The current distribution over the conducting surface is determined via matrix inversion.

The manner in which the structure is subsectioned is very important in any numerical analysis approach. Likewise the basic current distribution chosen for the subsections drastically affects the amount and difficulty of calculations. These methods will yield approximate results, the quality of the approximation depending on the amount of effort (and computer time) one is willing to devote to the problem.

As will be seen symmetry may simplify considerably the number of calculations involved. In some cases one may want to take advantage of symmetry; in other cases it may be simpler to ignore it. It appears that one must trade some formulation time for computer time. Is the tradeoff worthwhile? The answer to this question will depend on the extent of the computations. In reducing the number of unknowns, one

increases the analysis time but reduces computer programming time and computer running time.

II. METHOD OF ANALYSIS

A. METHOD OF MOMENTS

The method of moments has been widely explained in the literature. The interested reader may refer on this subject to References 5, 6 and 7.

B. PIECEWISE SINUSOIDAL BASIS SETS

The physical problem may be represented by many different operator equations, and a suitable one must be chosen. There are also an infinite number of sets of expansion functions and testing functions that may be chosen.

Intuitively, the more nearly the expansion set resembles the actual form of the current distribution, the fewer the terms required to accurately represent the current. In addition, certain types of basis functions may reduce many time-consuming numerical operations incorporated in approximations. The piecewise-sinusoidal basis set exhibits these qualities. The objective is to represent the current distribution, over individual subsections of a domain with expansion functions that possess greater curve-fitting potential than do flat pulses and yet lead to well-conditioned matrices in approximate solution procedures. The application of piecewise-sinusoids in Galerkin's method and the method of moments to electromagnetic field problems is known as the Piecewise-Sinusoidal Reaction Matching Technique.

C. PIECEWISE-SINUSOIDAL REACTION MATCHING TECHNIQUE. SURFACE MODEL

The reaction concept and its application has been discussed by Rumsey [Ref. 8], Cohen [Ref. 9], Harrington [Ref. 10] and Richmond [Ref. 11].

The following material has been previously presented by Richmond and Wang [Ref. 3]; it is presented here for completeness.

Consider the exterior scattering problem illustrated in Figure 1. In the presence of a dielectric or conducting body, the impressed electric and magnetic currents ($\underline{J}_i, \underline{M}_i$) generate the electric and magnetic field intensities ($\underline{E}, \underline{H}$). For simplicity let the exterior medium by free space.

From the surface-equivalence theorem of Schelkunoff, the interior field will vanish (without disturbing the exterior field) if the following surface-current densities are introduced:

$$\underline{J}_s = \hat{n} \times \underline{H} \tag{1}$$

$$\underline{M}_s = \underline{E} \times \hat{n} \tag{2}$$

on the closed surface s of the scatterer. (The unit vector $\hat{n}$ is directed outward on s.) In this situation, illustrated in Figure 2, it is possible to replace the scatterer with free space without disturbing the field anywhere.

By definition, the incident field ($\underline{E}_i, \underline{H}_i$) is generated by ($\underline{J}_i, \underline{M}_i$) in free space, and the scattered field is

$$\underline{E}_s = \underline{E} - \underline{E}_i \tag{3}$$

$$\underline{H}_s = \underline{H} - \underline{H}_i . \tag{4}$$

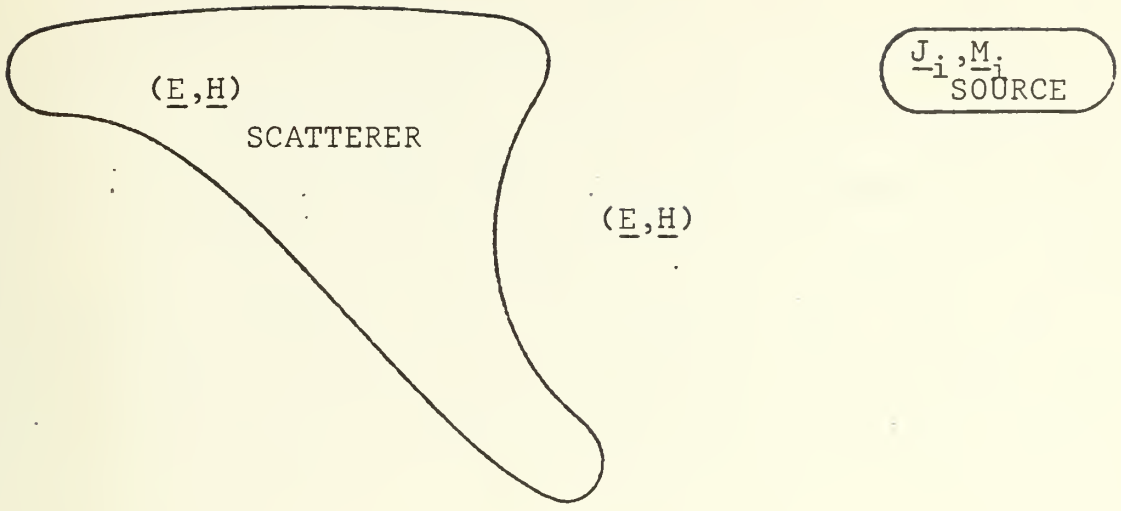

Figure 1. The Source ($\underline{J}_i$,$\underline{M}_i$) Generates the Field ($\underline{E}$,$\underline{H}$) with Scatterer.

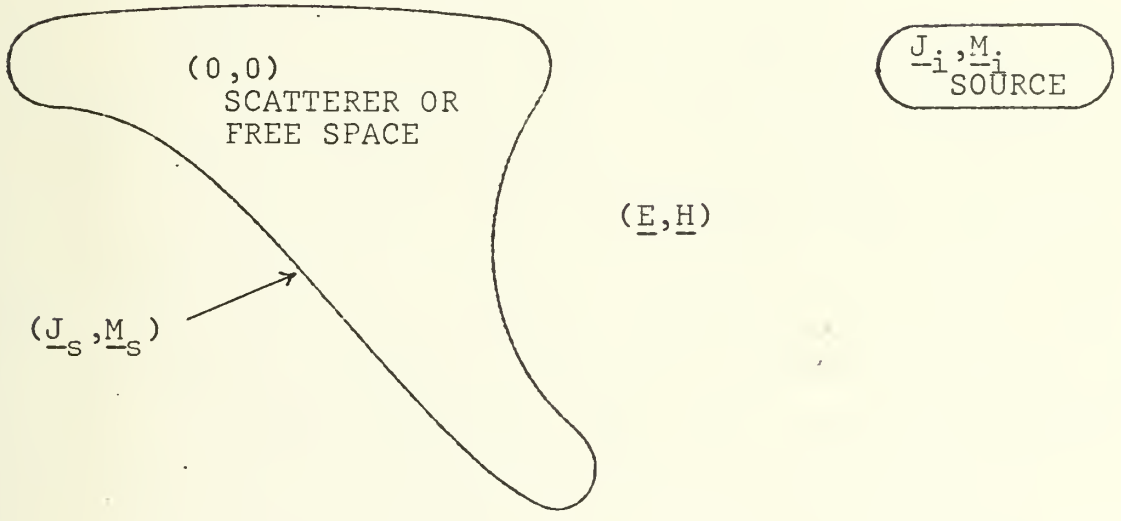

Figure 2. The Interior Field Vanishes When the Currents ($\underline{J}_S$,$\underline{M}_S$) are Introduced on the Surface of the Scatterer.

When the surface current ($\underline{J}_s$,$\underline{M}_s$) radiates in free space, it generates the field ($\underline{E}_s$,$\underline{H}_s$) in the exterior and ($-\underline{E}_i$,$-\underline{H}_i$) in the interior region. This result, illustrated in Figure 3, is deduced from Figure 2 and the superposition theorem.

With the scatterer replaced by free space, it can be noted in Figure 2 that the interior region has a null field. As shown in Figure 4, by placing an electric test source $\underline{J}_t$ in this region it is found from the reciprocity theorem that

$$\oint\!\!\!\!\!\!\diagup_s (\underline{J}_s \cdot \underline{E}_t - \underline{M}_s \cdot \underline{H}_t) ds + \iiint (\underline{J}_i \cdot \underline{E}_t - \underline{M}_i \cdot \underline{H}_t) dv = 0 \qquad (5)$$

where ($\underline{E}_t$,$\underline{H}_t$) is the free space field of the test source. In words, Equation (5) states that the interior test source has zero reaction with the other sources. This "zero reaction theorem" was developed by Rumsey [Ref. 8].

Equation (5) is the integral equation for the scattering problem, and the objective is to use this equation to determine the surface current distribution $\underline{J}_s$ and $\underline{M}_s$. To accomplish this, these functions are expanded in finite series yielding a finite number N of unknown expansion constants. Next N simultaneous linear equations are obtained to permit a solution for these constants. One such equation is obtained from Equation (5) each time a new test source is set up.

If the scatterer is a perfect conductor, the magnetic current $\underline{M}_s$ vanishes. Assuming a finite conductivity and using the impedance boundary condition

$$\underline{M}_s = \underline{Z}_s \, \underline{J}_s \times \hat{n} \qquad (6)$$

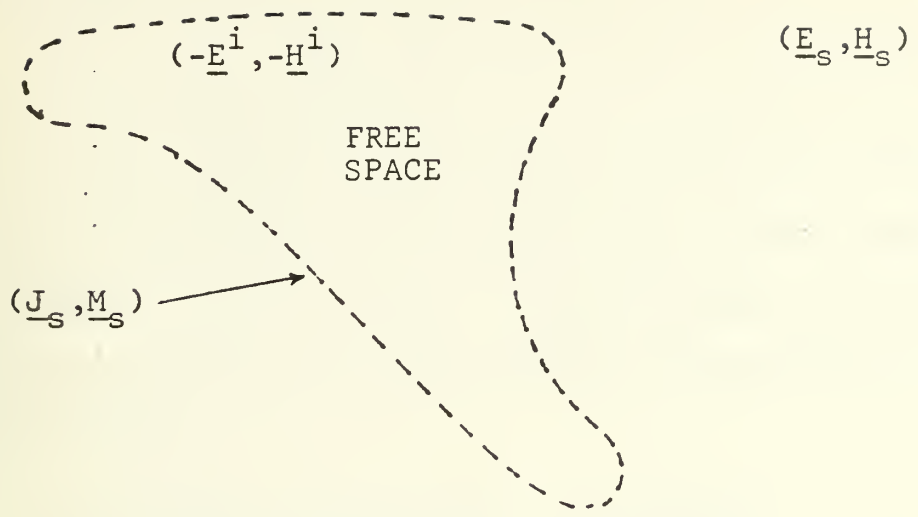

Figure 3. The Exterior Scattered Field may be Generated by $(\underline{J}_s, \underline{M}_s)$ in Free Space.

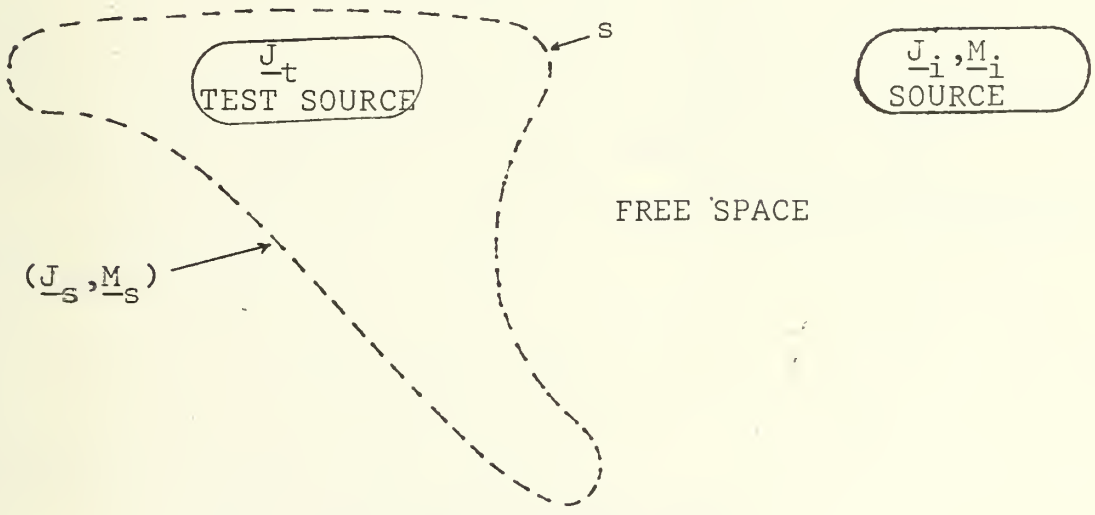

Figure 4. An Electric Test Source $\underline{J}_t$ is Positioned in the Interior of the Scattering Region.

where $\underline{Z}_s$ denotes the surface impedance equation (5) yields

$$-\oint\!\!\!\!\!\!\diagup_s J_s \cdot [\underline{E}_t - (\hat{n} \times \underline{H}_t) Z_s] ds = \iiint (\underline{J}_i \cdot \underline{E}_t - \underline{M}_i \cdot \underline{H}_t) dv. \quad (7)$$

For two-dimensional problems involving arbitrary scatterers, $\underline{J}_s$ and $\underline{M}_s$ are functions only of the position on the surface of the scatterer. If $\underline{M}_i$ vanishes and denoting (E_m, H_m) as the free-space field of test-source m, Equation (7) yields

$$-\iint_s \underline{J}_s \cdot [\underline{E}_m - (\hat{n} \times \underline{H}_m) Z_s] ds = \iint J_i \cdot \underline{E}_m ds. \quad (8)$$

Now representing the electric current distribution as follows:

$$\underline{J}_s = \sum_{n=1}^{N} I_n \underline{J}_n \quad (9)$$

where the complex constants I_n are samples of the function $\underline{J}_s$. The vector functions $\underline{J}_n$ are known as basis functions. Basis functions $\underline{J}_n$, and testing (weighting) sources $\underline{J}_m$ with unit current density at their terminals are used.

From Equations (8) and (9) the following simultaneous linear equation is obtained

$$\sum_{n=1}^{N} I_n C_{mm} = A_m \quad (10)$$

with m = 1,2,3,...,N, where

$$C_{mm} = -\iint_n \underline{J}_n . [\underline{E}_m - (\hat{n} \times \underline{H}_m) Z_s] ds$$

$$= -\iint_m \underline{J}_m \cdot \underline{E}_n \, ds \quad (11)$$

$$A_m = \iint_i \underline{J}_i \cdot \underline{E}_m \, ds = \iint_m \underline{J}_m \cdot \underline{E}_i \, ds \quad (12)$$

The integrations in Equations (11) and (12) extend over the region where the integrand is non-zero. Region "m" covers the interior test source, $\underline{J}_m$, and region "n" is that portion of the surface s covered by the expansion function $\underline{J}_n$. The first and the second integrals in Equation (11) are related by the reciprocity theorem, where E_n is the free-space field generated by $\underline{J}_n$ and the associated magnetic current $\underline{M}_n$.

D. UNIDIRECTIONAL CURRENT MODEL

A two-dimensional surface dipole located on the y-z plane is illustrated in Figure 5(a). This source is an electric surface-current density with height 2D and width w. The surface current density is given by

$$\underline{J}_{(z)} = \frac{\sin K(D-z)}{\sin KD}\ \hat{z} \qquad \text{for } 0 < z < D \qquad (13)$$

$$\underline{J}_{(z)} = \frac{\sin K(D+z)}{\sin KD}\ \hat{z} \qquad \text{for } -D < z < 0 \qquad (14)$$

where $K = 2\pi/\lambda$.

As illustrated in Figure 5(b), the current density is assumed to be piecewise-sinusoidal in the z-direction, with period equal to λ, vanishing at the edges $z = D$ and $z = -D$, and equal to unity at the center. From Figure 5(c) it can be seen that the current density is assumed to be uniformly distributed in the tranverse direction.

The dipole current distribution, Equations (13) and (14), will be used as the basis functions ($\underline{J}_n$ in Equation (9)) for expanding the unknown current distribution induced on a conducting surface. Also, surface dipoles will be

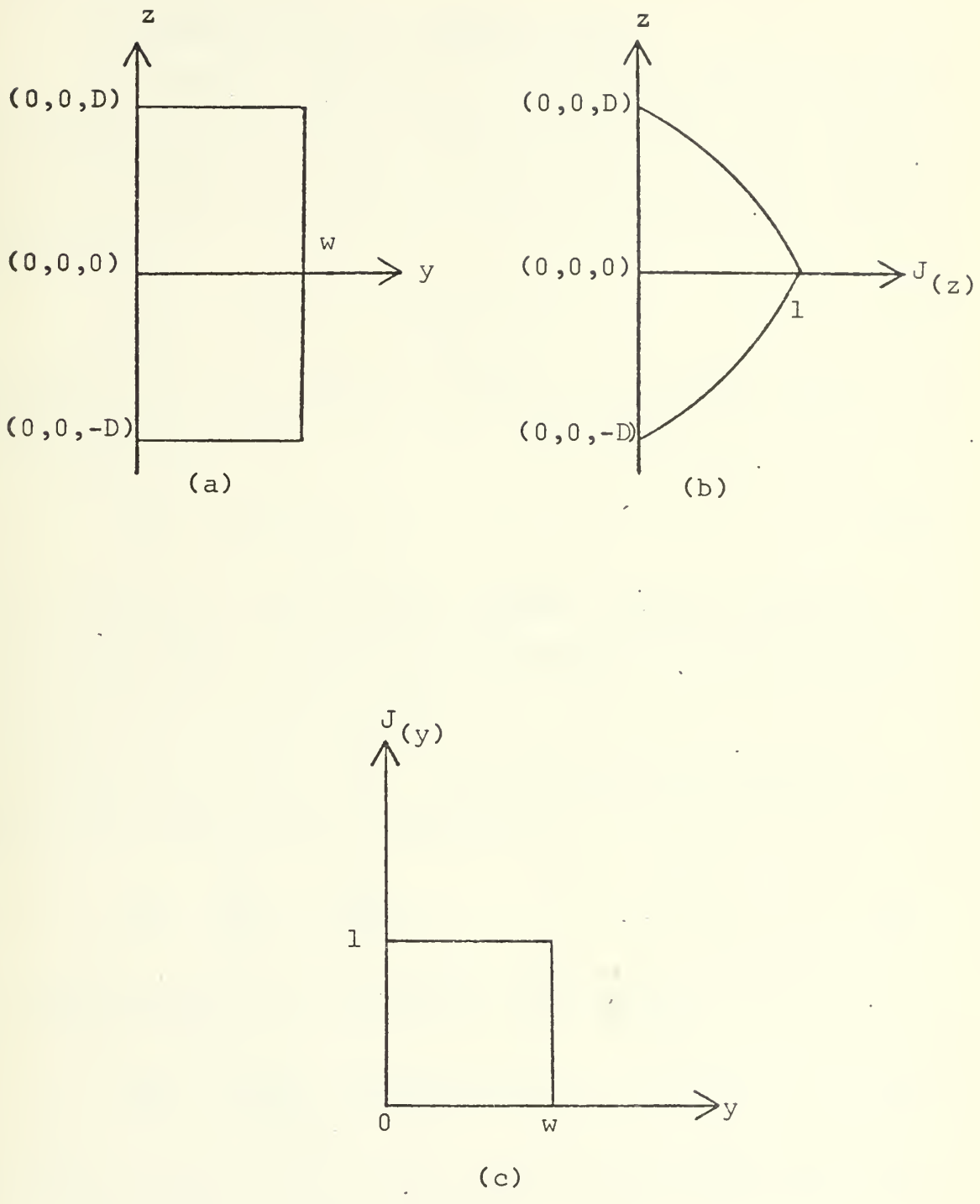

Figure 5. An Electric Surface Dipole and Its Current Density Distribution.

employed as test sources with the reaction concept to solve the integral equation.

1. Calculation of the Coupling Term

The complex number C_{mm} in Equation (11) represents the mutual coupling between two sources. Let <m,n> denote the mutual coupling between sources, then Equation (11) can be written as

$$C_{mn} = -\langle m,n \rangle = -\iint_m \underline{J}_m \cdot \underline{E}_n \, ds \tag{15}$$

Relating the mutual coupling between two sources to the circuit parameters [Ref. 3]

$$C_{mn} = V_{mn} I_{on} \tag{16}$$

where V_{mn} is the open circuit terminal voltage induced at source m by source n, and I_{on} is the short circuit terminal current induced at source n.

The surface dipole self impedance has been defined [Ref. 3] with the induced-emf formulation:

$$Z_{mm} = \frac{V_{mm}}{I_{om}} = \frac{C_{mm}}{I_{om} I_{om}} . \tag{17}$$

From Equation (15), Equation (17) yields

$$Z_{mm} = \frac{-1}{I_{om} I_{om}} \iint_m \underline{J}_m \cdot \underline{E}_m \, ds. \tag{18}$$

where $\underline{J}_m$ is the surface-current density of source m and $\underline{E}_m$ is its free space electric field.

The mutual impedance between two surface dipoles is defined [Ref. 3] by

$$Z_{mm} = \frac{-1}{I_{om} I_{on}} \iint_m \underline{J}_m \cdot \underline{E}_n \, ds. \qquad (19)$$

The evaluation of the integrals in Equations (18) and (19) requires use of numerical integration techniques. K. Khemayodhin has developed a computer program to evaluate these integrals. Details and results are shown in his Engineer's Degree Thesis to be presented to the Electrical Engineering Department, Naval Postgraduate School, in December 1974. His computer program has been used in this thesis to calculate the self and mutual coupling between surface dipoles.

Table I lists the self impedance of a center-fed two-dimensional dipole as a function of size. Table II lists the mutual impedance between the two-dimensional dipoles shown in Figure 7 as a function of their relative position.

From Equations (17) and (19) the mutual coupling is derived as

$$C_{mn} = I_{om} \, I_{on} \, Z_{mn}. \qquad (20)$$

For the dipole shown in Figure 5, I_{om} is the total current at z = 0. Since J = 1 at the center of the dipole

$$I_{om} = \int_0^w \underline{J} \, dy = w. \qquad (21)$$

For identical dipoles and from Equation (21), Equation (20) yields

$$C_{mn} = w^2 \times Z_{mn}. \qquad (22)$$

Table I. Self Impedance of Center-Fed Two-Dimensional Dipole Shown in Figure 6.

w/λ	R(1,1)	X(1,1)
0.2	7.91	- 68.06
0.3	17.91	- 33.08
0.4	32.47	- 14.54
0.5	53.11	- 4.67

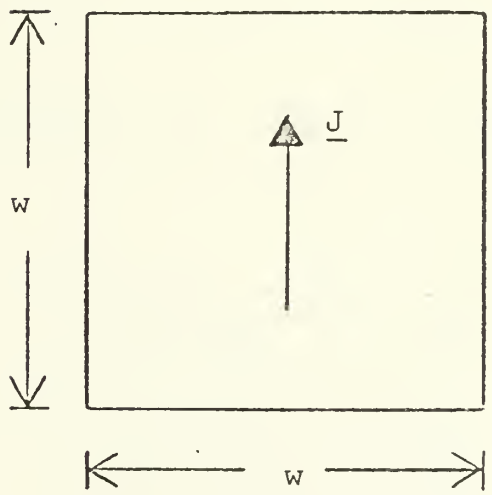

Figure 6. Two-Dimensional Dipole.

Table II. Mutual Impedance of Center-Fed Two-Dimensional Dipoles Shown in Figure 7.

z/λ \ y/λ	0.0	0.25	0.50	0.75
0.0	67.3+j13.9	38.9-j22.2	-8.5-j26.6	19.2+j4.2
0.25	53.3+j59.7	29.4-j8.6	-9.4-j19.7	-15.6+j6.4
0.50	23.5+j6.3	10.0-j9.2	-9.5-j6.6	-7.2+j8.9
0.75	1.1-j7.9	-2.9-j5.9	-5.9+j1.7	0.9+j7.0

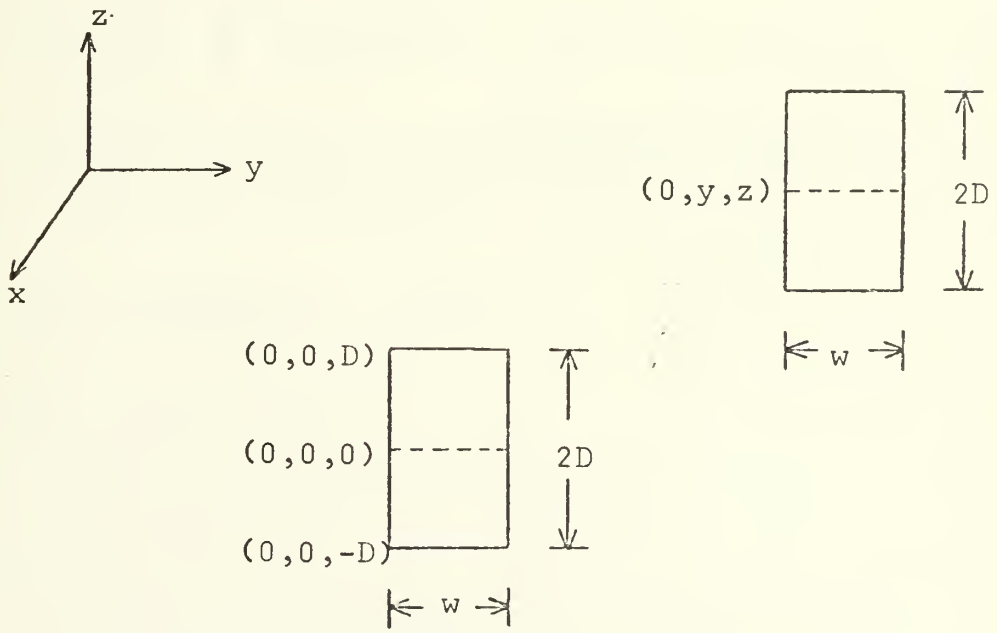

Figure 7. Coupled Two-Dimensional Dipoles with D = 0.25λ and w = 0.25λ.

2. Calculation of the Excitation Column

In the matrix equation $C_{mn}\ I_n = A_m$, the complex quantities A_m form the excitation column. Physically, A_m is the reaction between the impressed source and the surface dipole m. If the impressed source is an electric line source with current density $\underline{J}_i$, Equation (12) reduces to

$$A_m = \iint_m \underline{J}_m \cdot \underline{E}_i \, ds. \tag{23}$$

Assuming a line source located at a great distance from the surface, the incident field may be regarded as a plane wave with

$$\underline{E}_i = E_o \, e^{jKx}. \tag{24}$$

For $E_o = 1$ and at $x = 0$, $\underline{E}_i = 1$. For the two-dimensional dipole shown in Figure 5(a), Equation (23) reduces to

$$A_m = \int_o^w \int_o^{2D} \underline{J}_m \, dz \, dy. \tag{25}$$

Using the surface current density assumed in Equation (13) and (14), Equation (25) yields

$$A_m = \frac{2\ w}{K \sin KD} (1 - \cos KD). \tag{26}$$

E. GENERAL CURRENT MODEL

A two-dimensional surface quadrupole located on the y-z plane is illustrated in Figure 8(a). This source is an electric surface-current density with height 2D and width 2 w. The surface current density is given by

$$\underline{J}_{(z)} = \frac{\sin K(D-z)}{\sin KD} \hat{z} \quad \text{for} \quad 0 < z < D \tag{27}$$

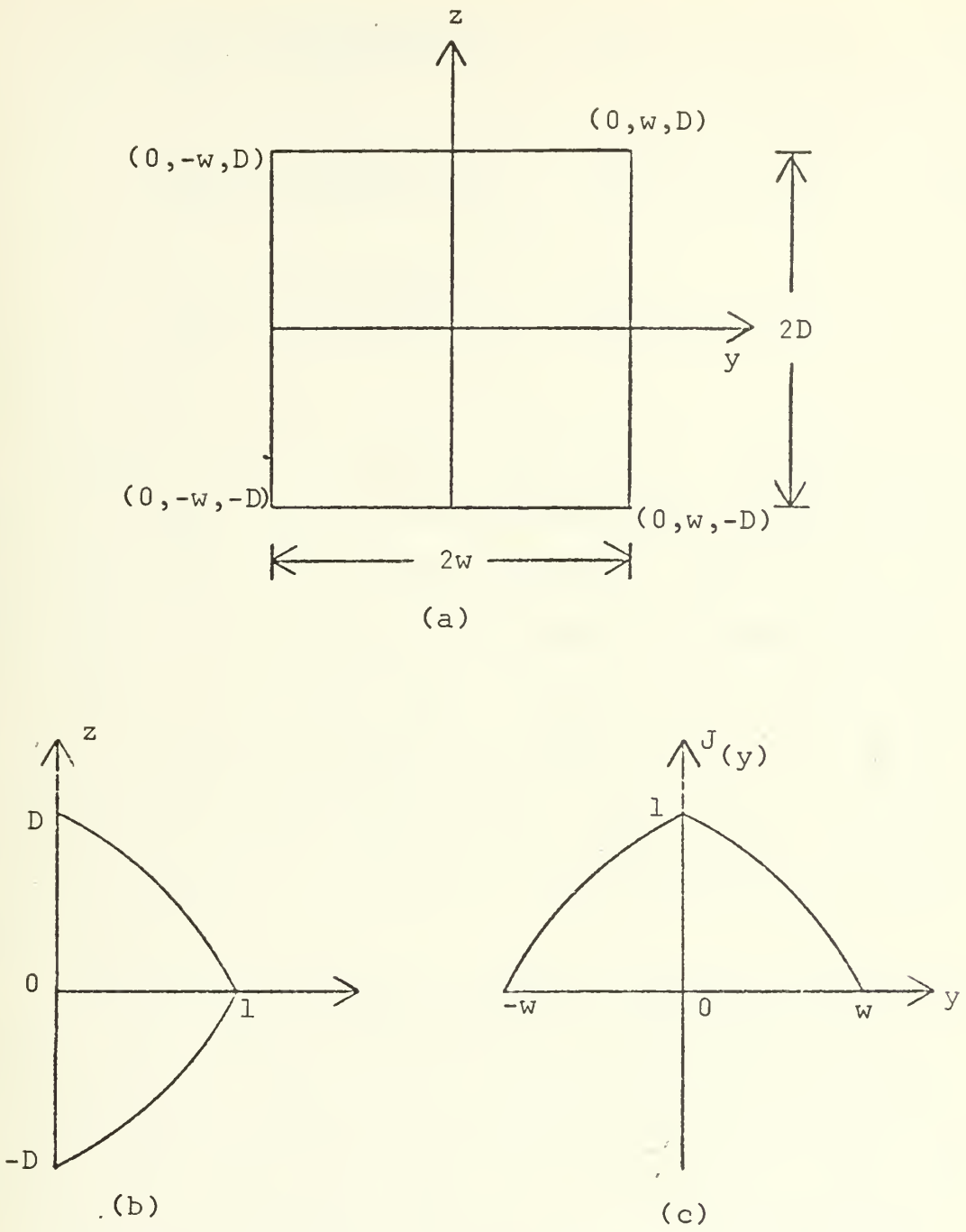

Figure 8. A Two-Dimensional Electric Quadrupole and its Current Density Distribution.

$$\underline{J}_{(z)} = \frac{\sin K(D+z)}{\sin KD}\,\hat{z} \qquad \text{for } -D < z < 0 \qquad (28)$$

$$\underline{J}_{(y)} = \frac{\sin K(w-y)}{\sin Kw}\,\hat{y} \qquad \text{for } 0 < y < w \qquad (29)$$

$$\underline{J}_{(y)} = \frac{\sin K(w+y)}{\sin K\,w}\,\hat{y} \qquad \text{for } -w < y < 0 \qquad (30)$$

where $K = 2\pi/\lambda$.

As illustrated in Figure 8(b) and (c), the current density is assumed to be piecewise-sinusoidal in the y-direction and z-direction, with period equal to λ, vanishing at the edges and equal to unity at the center. Comparing this structure with the one used in the Unidirectional Current Model it can be appreciated that the quadrupole is a combination of the dipoles used in the former. Its current distribution will be the product of the two functions shown in Figures 8(b) and 8(c).

K. Khemaydhin has also developed a computer program to evaluate the current distribution on conducting bodies of arbitrary shape. Details are contained in his aforementioned thesis. This computer program has been used in this thesis to calculate the current distribution in two-dimensional structures when current in two directions was assumed.

III. COMPUTER PROGRAM. DISCUSSION, DESCRIPTION AND RESULTS

This section is concerned with the discussion and description of the computer programs used to find the current distribution in the several two-dimensional structures to be treated. There are a number of refinements which can be introduced to improve the accuracy of the solution, as well as to increase the effectiveness of the use of the computer memory. The principles involved are simple in concept; in each case an integral equation is replaced with a matrix equation, which is inverted to solve for the unknown source function.

A. UNIDIRECTIONAL CURRENT MODEL

In the solution for current distribution in the several two-dimensional structures in which only one direction of current was allowed, it was assumed that a line source is located at a great distance from the surface so that the incident field may be regarded as a plane wave. The plane wave is assumed to be incident at broadside and in the z-direction.

The number of subsections is, of course, a very important quantity in any Numerical Analysis Approach. One of the easiest methods of improving accuracy is merely to increase the number of subsections, but increasing the number of subsections increases the number of unknowns, the time of computer programming, the computer running time and the computer memory space. Thus it appears that it is a tradeoff between

the extent of computations and the accuracy of the solution desired.

For all the structures solved, the surface was divided into an integer number of equal two-dimensional dipoles. Although this method of segmentation gives an equal resolution at the sharp edges (where the current density is varying very rapidly) as well as in the center of the surface (where the current density is almost constant), it allows the use of symmetry for the calculations of the coupling terms. The use of symmetry, as explained in each of the particular cases, has saved considerable computational time.

1. The Rectangular Plate

The first problem solved was the rectangular plate, for which Richmond and Wang [Ref. 3] have previous results. The rectangular plate, as shown in Figure 9, was divided into ninety overlapping dipoles. The current density distribution was found with Computer Program 1 listed in Appendix A. Its description is as follows: the program written for a rectangular shaped structure is a general program applicable for different methods of segmentation. The only restriction is that the segments (dipoles) must be equal. The number of dipoles is limited by the size of the matrix which the inverting matrix subroutine can handle, usually 100. Subroutine CMTRIN, modified to handle matrices up to 200 by 200, was used in this program.

The way to describe the rectangular plate is by entering the following parameters: (a) L1 is the number of dipoles in a row (30 in Figure 9); (b) L3 is the number of

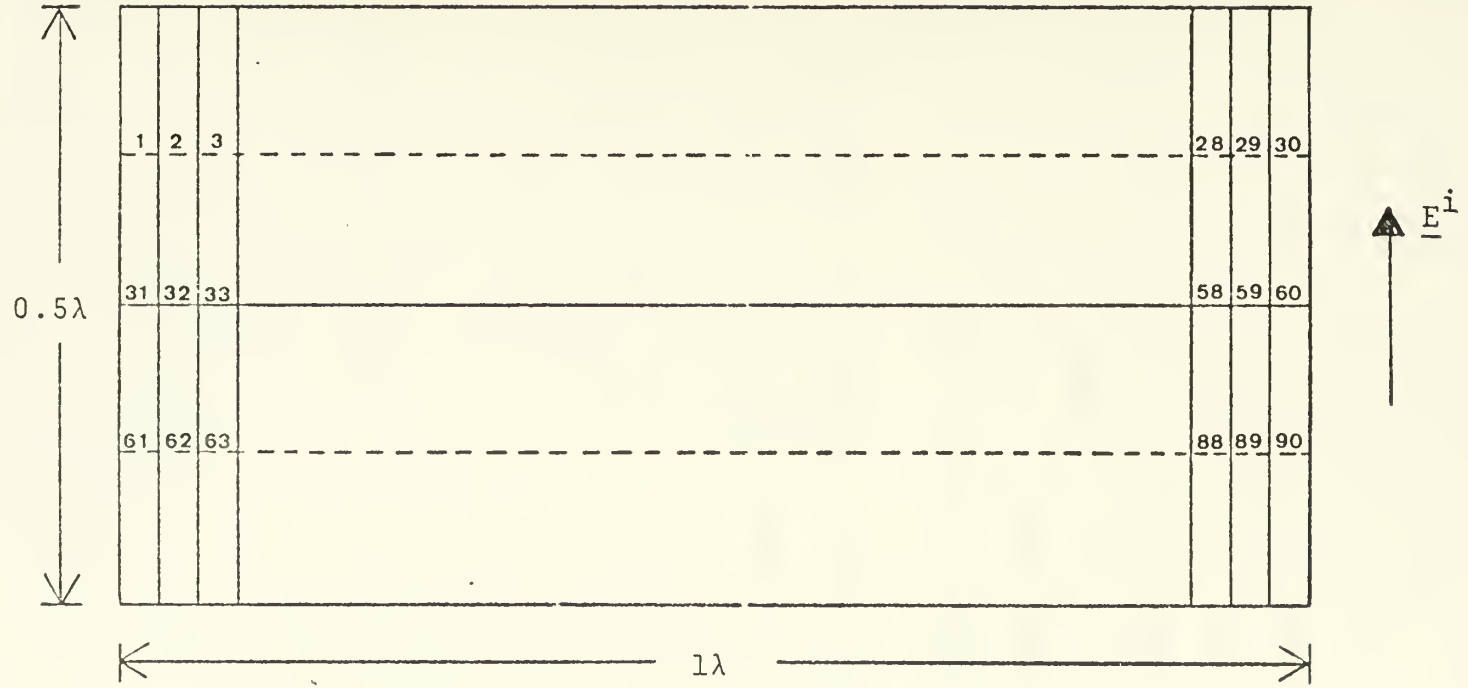

Figure 9. Rectangular Plate Segmented in 90 Overlapping Dipoles. Plane Wave Incident at Broadside.

rows of dipoles (3 in Figure 9); (c) L7 is the total number of dipoles in the surface (90 in Figure 9); (d) D is the half-length of the dipole (see Figure 5(a)); (e) w is the width of the dipole (see Figure 5(a)).

DO LOOPS 100, 200, 300, and 400 generate the coordinates of the source dipole and the test dipole as shown in Figure 7. Each dipole is at one time a test dipole, with all the other dipoles becoming source dipoles. In calculating the self impedance, the Complex Function ZSDPAR provides a 0.001λ separation between dipoles and calculates this closely-coupled case of mutual impedance as the self impedance.

The number of times the calculation of the coupling between dipoles has to be performed depends on the number of dipoles on the surface. The time each calculation of the coupling term takes in the IBM 360/67 computer has been estimated to be an average of 1.6 seconds. To perform the 8100 calculations for the rectangular plate would take 216 minutes of computer time. However, noticing that the coupling between dipoles depends only on their relative position, it is possible to apply some symmetry to the problem. Calculating only the first row of the coupling matrix, that is, the coupling between dipole 1 and all other dipoles in the surface will yield sufficient terms for filling the rest of the matrix. So, only 90 calculations of the coupling term need to be performed, reducing the computer time drastically to 2.4 minutes. DO LOOPS 450 and 466 perform the

symmetry comparison by comparing the relative position of the dipoles.

The calculation of the right hand side vector of Equation (10) is performed with the closed form of Equation (26).

The coefficient matrix is then inverted using subroutine CMTRIN.

DO LOOPS 2400 and 2500 perform the multiplication of the inverted matrix $[C(m,n)]^{-1}$ by the excitation column $[A(m)]$.

DO LOOP 3000 performs the calculation of the current density at each dipole and normalizes it to the Magnetic Field Intensity

$$\eta = \frac{E_z}{H_y} . \tag{31}$$

From Equation (24), $E_z = 1$, then

$$H_y = \frac{1}{\eta} . \tag{32}$$

The absolute value of the current density is plotted using the three-dimensional plot sub-program PLT3D1 and is shown in Figure 10.

2. The Square Plate

The two-dimensional square plate is shown in Figure 11. The structure was divided in 90 overlapping dipoles.

The current density distribution was found using Computer Program 1 following exactly the same procedure as in the rectangular plate. The only difference is in the size of the dipoles. For the square plate D = 0.25λ and

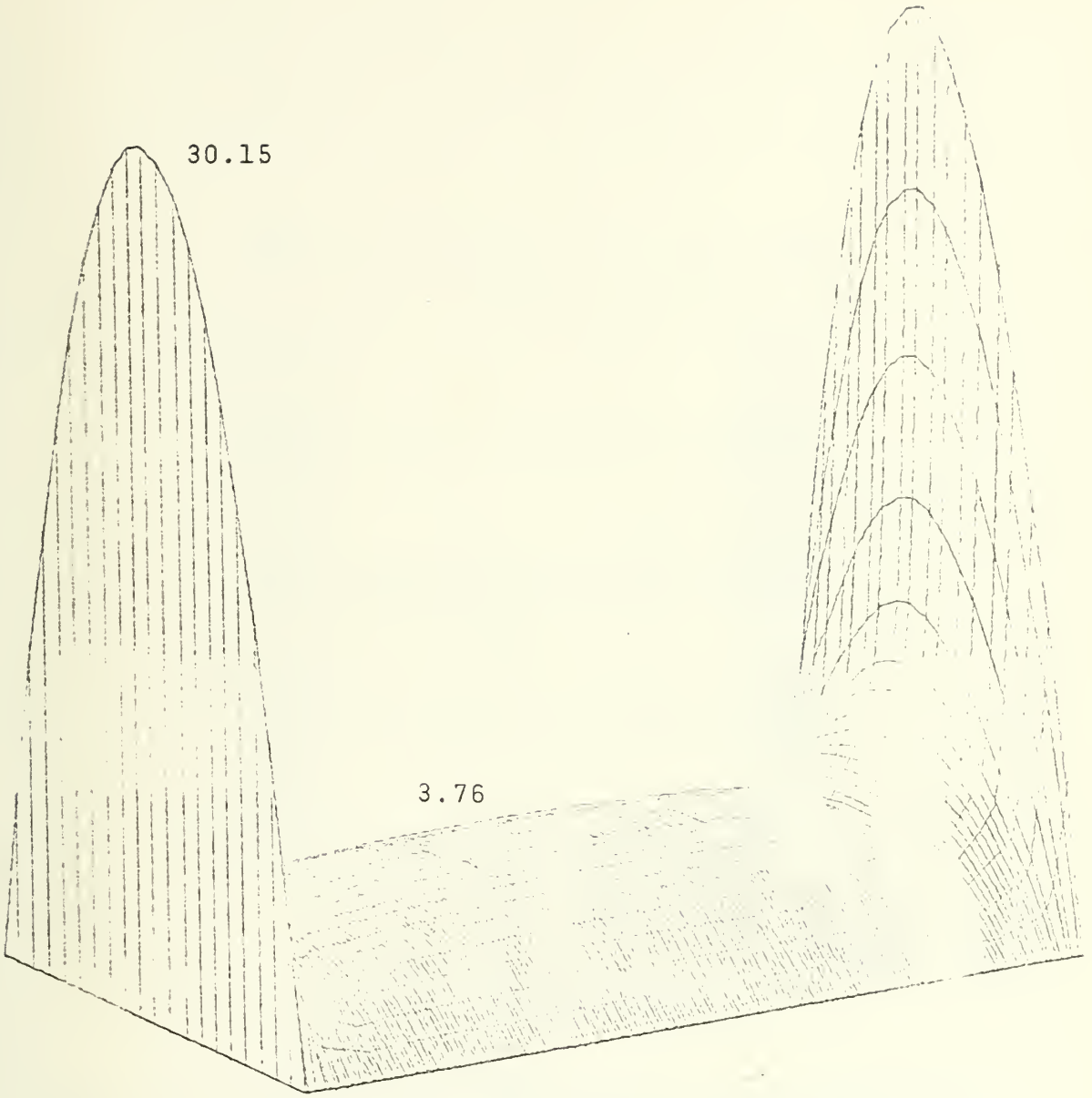

Figure 10. Rectangular Plate (1λ by 0.5λ) Magnitude of Induced Current.

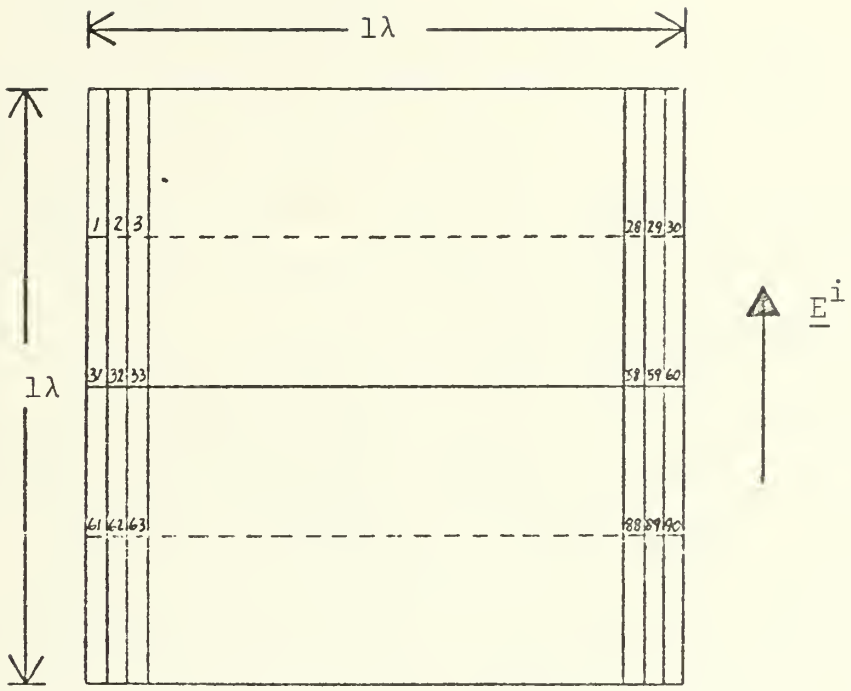

Figure 11. Square Plate Segmented in 90 Overlapping Dipoles. Plane Wave Incident at Broadside.

$w = 1/30\lambda$, instead of $D = 0.125\lambda$ and $w = 1/30\lambda$ as used in the rectangular plate.

The current density distribution is shown in Figure 12 and was plotted using the three-dimensional plot sub-program PLT3D1.

3. 'L'-Shaped Structure

The 'L'-shaped structure is shown in Figure 13. The structure was divided into 60 dipoles.

Computer Program 2 listed in Appendix A was used to solve the current density distribution for the 'L'-shaped structure. This is a general program applicable for different ways of segmentation of an 'L'-shaped structure. It has the same restrictions as Computer Program 1 (rectangular plate), in fact both programs are quite similar. Computer Program 2 assumes first that the surface is a squared surface and following the same procedure described in Computer Program 1, calculates the coupling between dipoles of the squared surface. The program has been designed in this way in order to be able to apply symmetry.

DO LOOPS 501 through 507 assign the corresponding coupling from the squared surface to the 'L'-shaped surface. Then, the same procedure as in Computer Program 1 is applied to calculate the right hand side vector, to invert the coefficient matrix, to multiply the inverted matrix by the right hand side vector and finally to calculate the current density at each dipole.

The magnitude of the induced current density is plotted using the three-dimensional plot sub-program PLT3D1 and is shown in Figure 14.

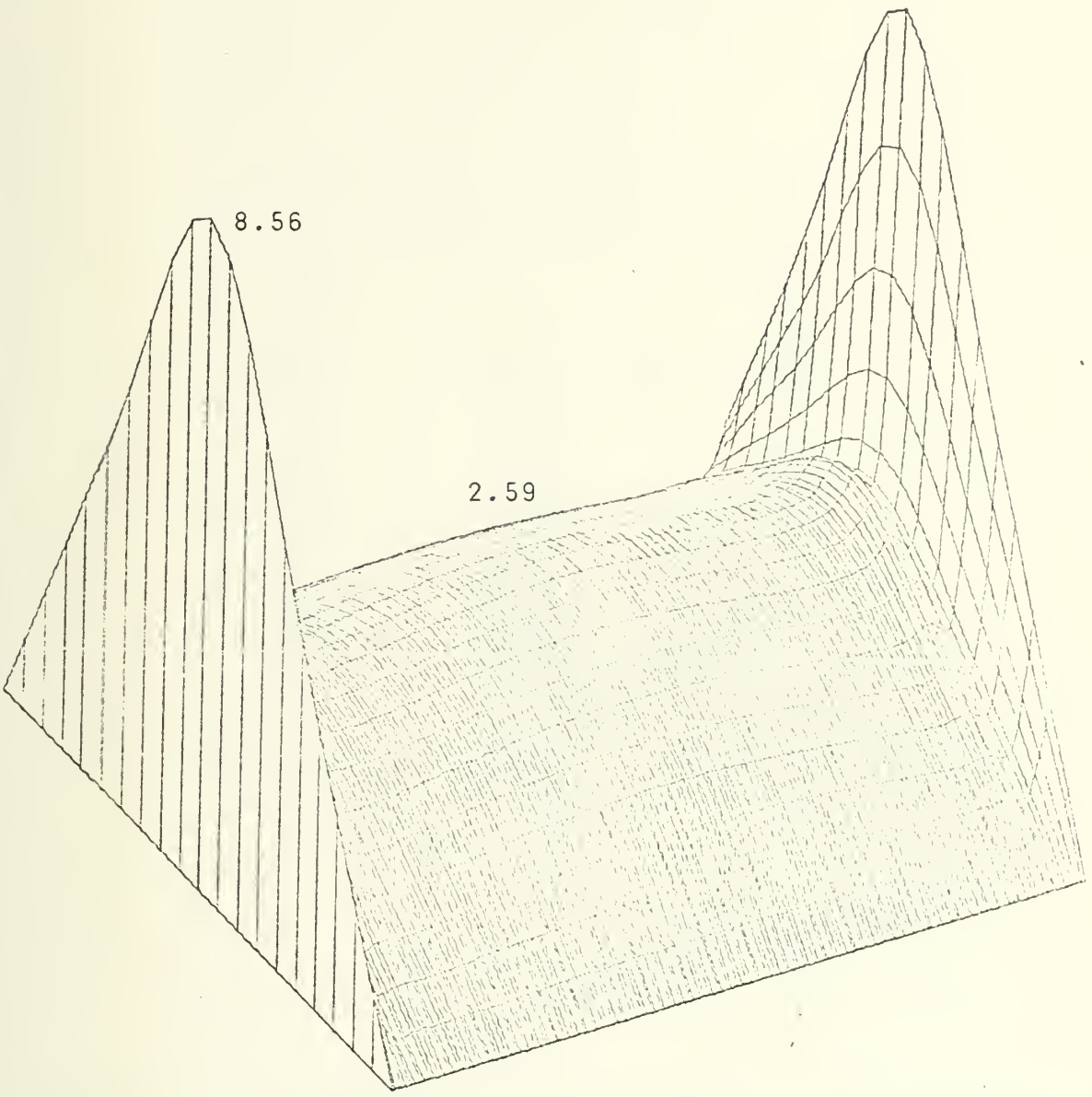

Figure 12. Square Plate (1λ by 1λ) Magnitude of Induced Current.

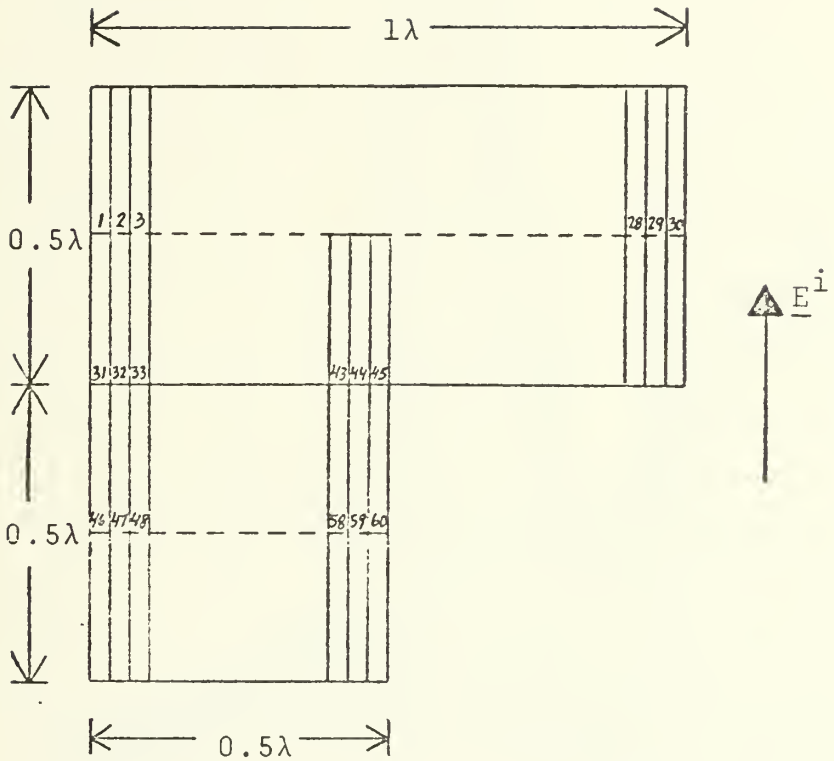

Figure 13. 'L'-Shaped Structure Segmented in 60 Overlapping dipoles. Plane Wave Incident at Broadside.

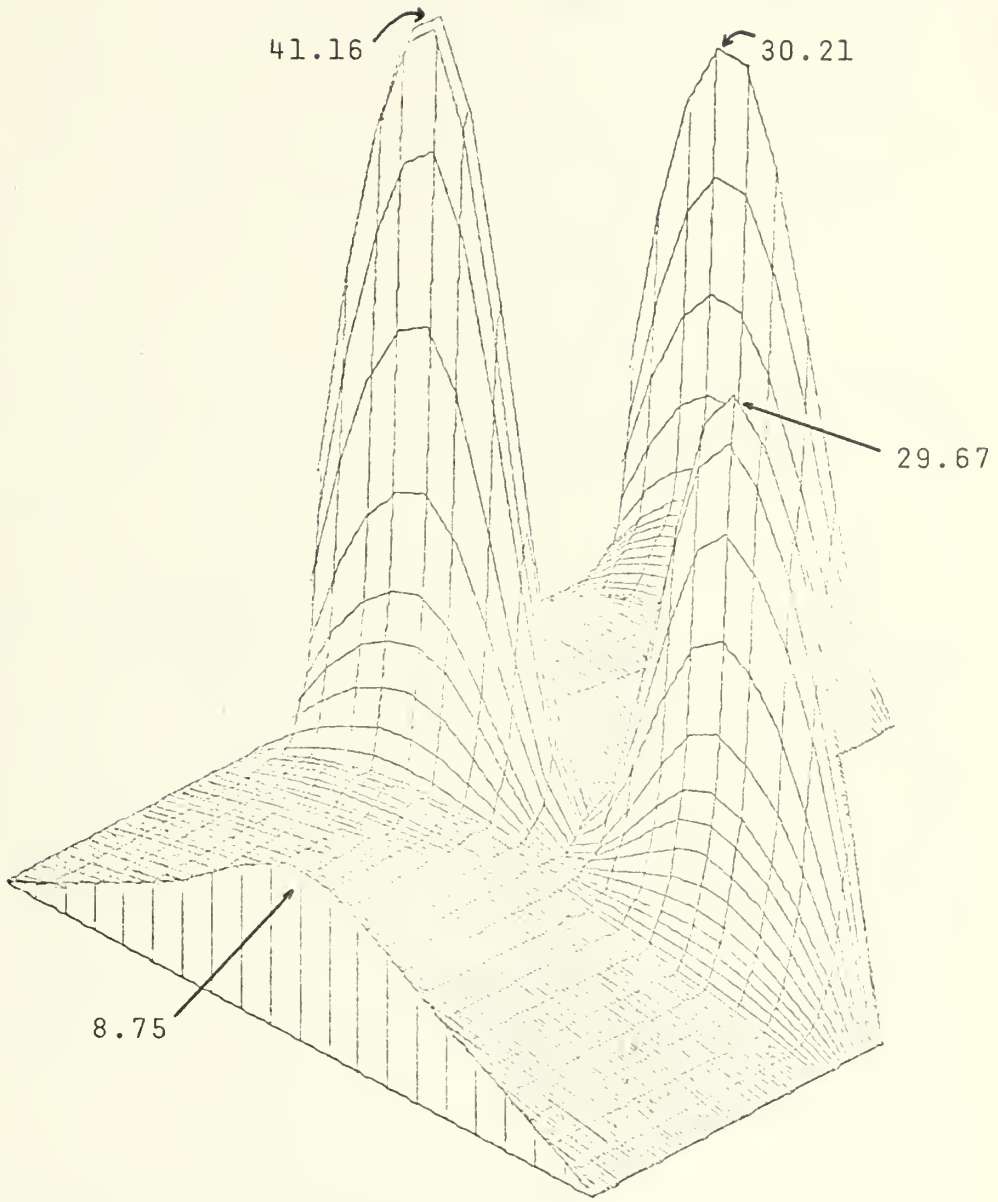

Figure 14. 'L'-Shaped Structure (1λ by 1λ) Magnitude of Induced Current.

4. The 'T'-Shaped Structure

The 'T'-shaped structure was segmented in 64 dipoles as shown in Figure 15.

Computer Program 3 listed in Appendix A was used to solve the current density distribution for the 'T'-shaped structure. The procedure is exactly the same that the one used in the 'L'-shaped structure. The differences are in the number of dipoles used and the width of the dipole (1/32 λ instead of 1/30 λ used in the 'L').

The current density distribution is shown in Figure 16 and was plotted using the three-dimensional plot subprogram PL3TD1.

5. The Two-Dimensional Cross

The two-dimensional cross was segmented in 80 overlapping dipoles as shown in Figure 17. Computer Program 4 listed in Appendix A was used to solve for its current density distribution. The procedure is exactly the same that the one used for the 'L'-shaped structure. The differences are in the number of dipoles used and the size of the dipoles. For the two-dimensional cross D = 1/8 λ and w = 1/16 λ.

The current density distribution is shown in Figure 18 and was plotted using the three-dimensional plot subprogram PL3TD1.

B. GENERAL CURRENT MODEL

For the solution of current distribution in the several two-dimensional structures in which two directions of current

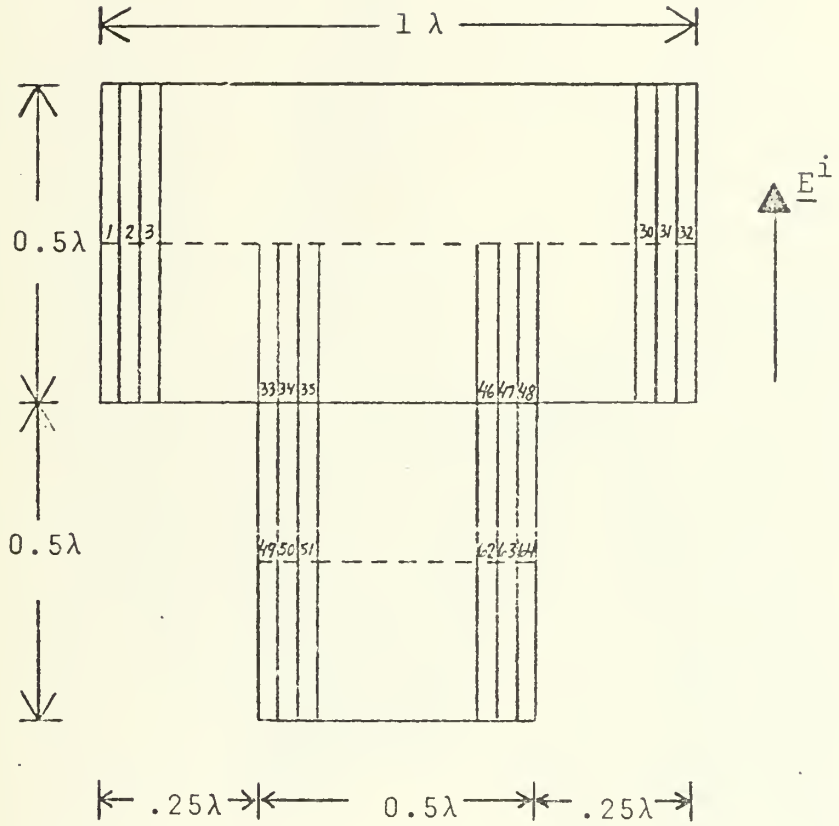

Figure 15. 'T'-Shaped Structure Segmented in 64 Overlapping Dipoles. Plane Wave Incident at Broadside.

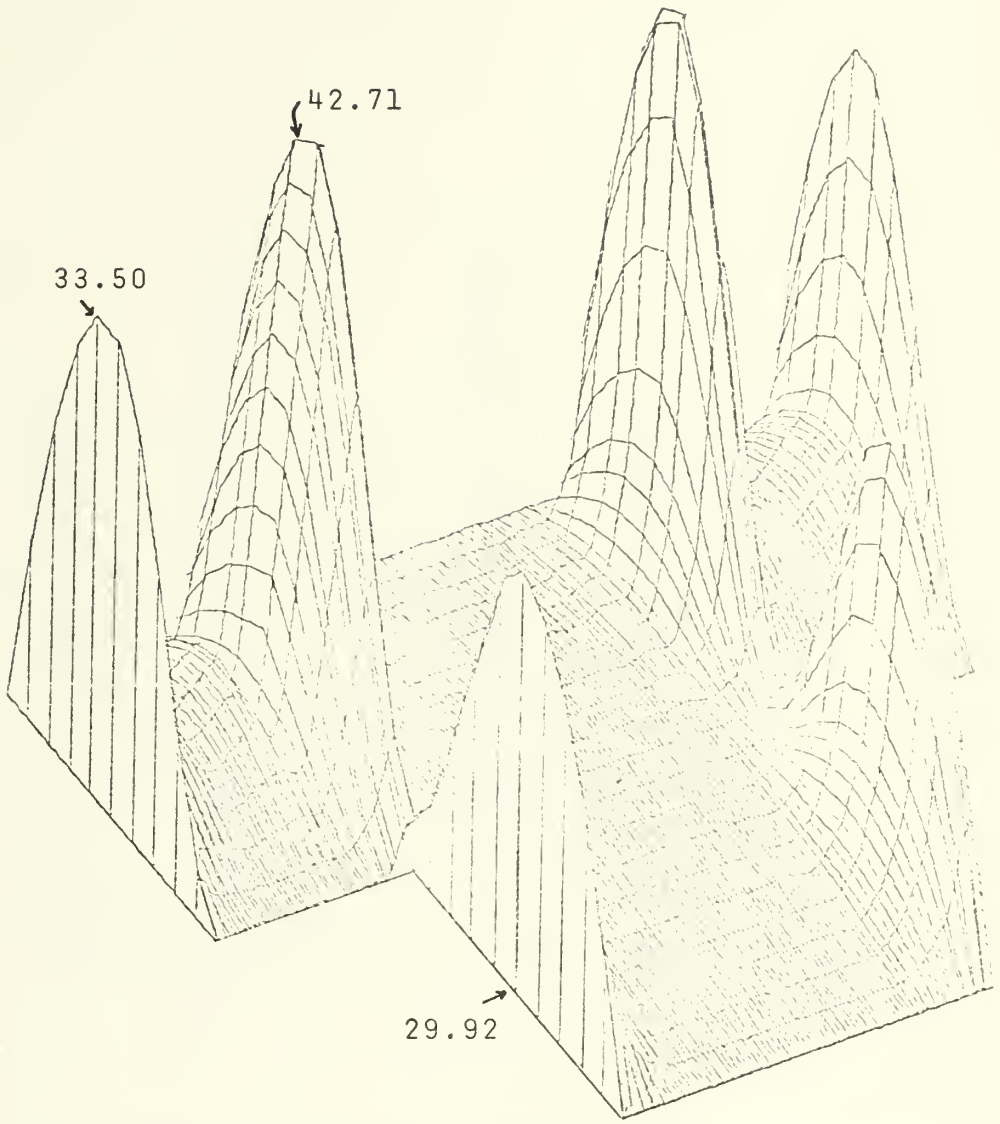

Figure 16. 'T'-Shaped Structure (1λ by 1λ) Magnitude of Induced Current.

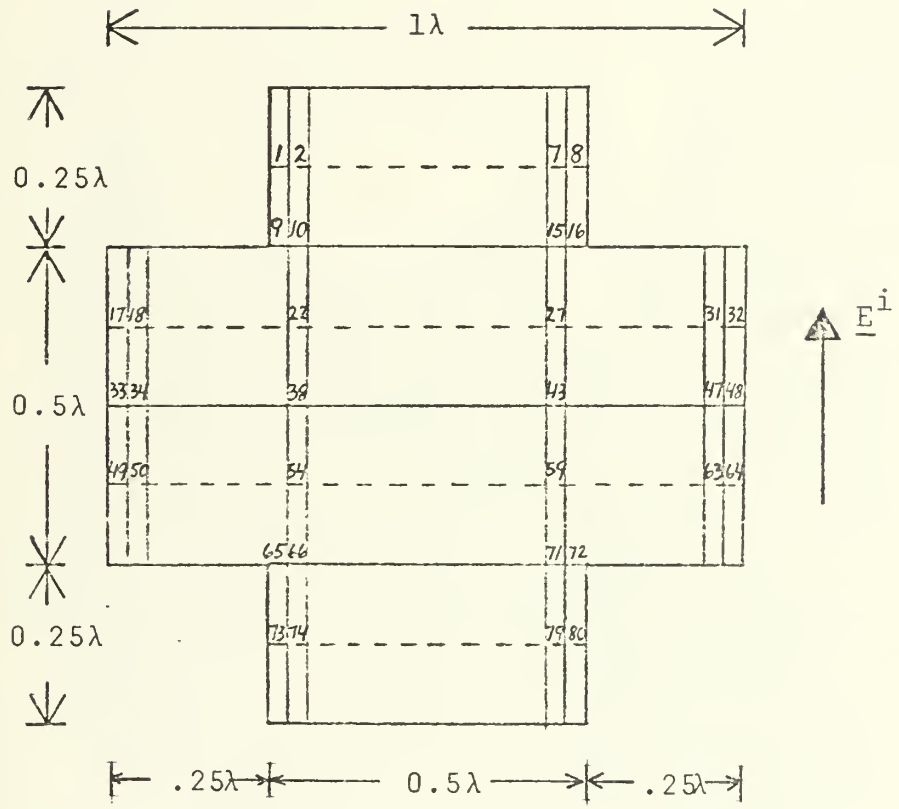

Figure 17. Two-Dimensional Cross Segmented in 80 Overlapping Dipoles. Plane Wave Incident at Broadside.

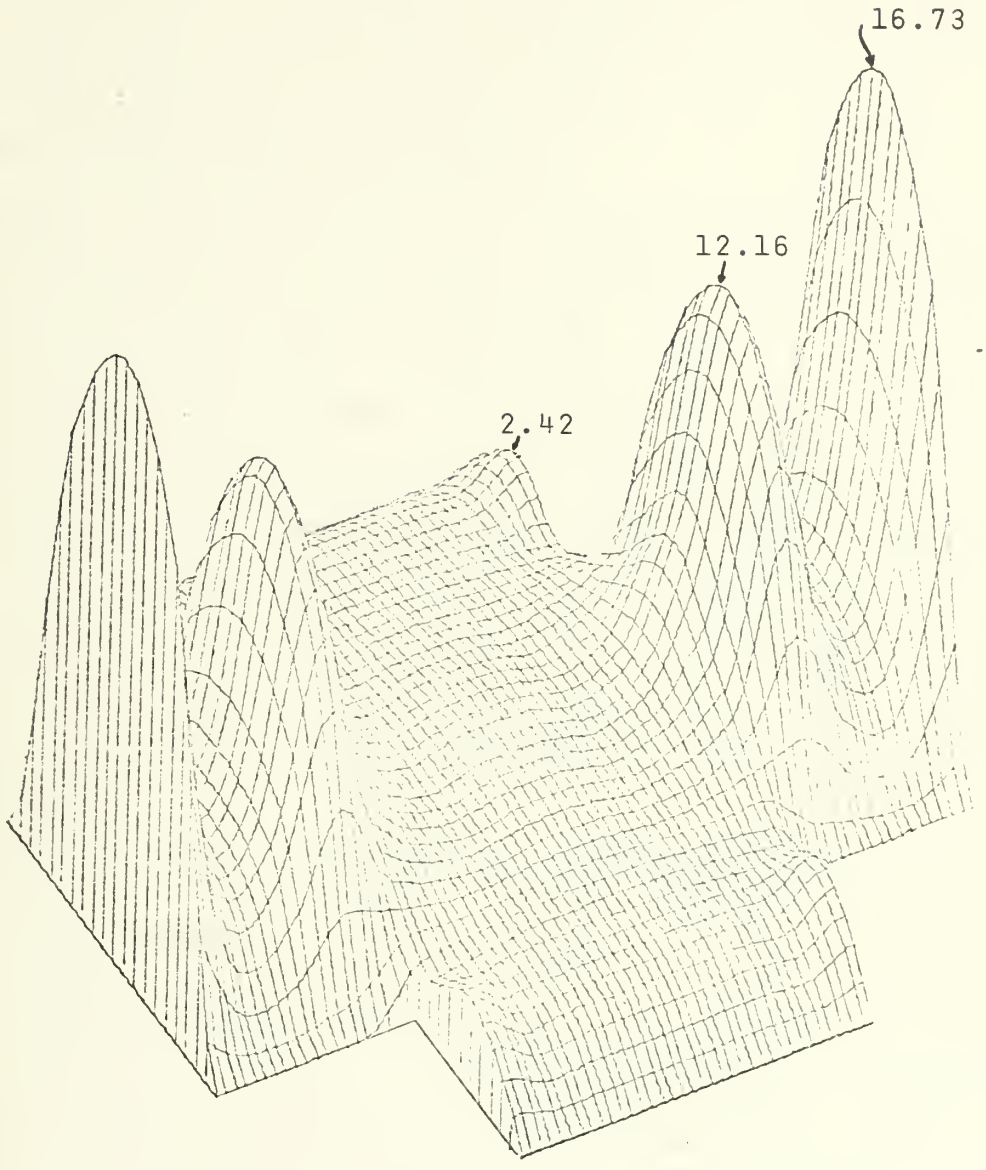

Figure 18. Two-Dimensional Cross Structure Magnitude of Induced Current.

was allowed, the Computer Program written by K. Khemayodhin was used. This thesis was concerned only with the design of the subroutines to generate the geometry of the structures. For all the solutions an electric field of 120π volts/meter incident at broadside was assumed.

Computer Program 5 as listed in Appendix A was used to generate the geometry of all the structures. This program generates a square plate of dimensions 1 λ by 1 λ. The difference in the particular structures that has been solved is the current path assumed. Thus, this program can be also used for the Unidirectional Current Model by only specifying currents in one direction. The reason for not using it in the Unidirectional Current Model is the much longer computer running time it takes, since symmetry considerations are not fully applied.

All the results have been plotted using the three-dimensional plot subprogram PL3TD1.

1. The Rectangular Plate

The structures of dimensions 1 λ by 0.5 λ was divided, as shown in Figure 19, in 32 surface (monopoles). Eight current paths were assumed in the z-direction and four in the y-direction. Figure 20 shows the magnitude of the induced current in the direction of the field. Figure 21 shows the magnitude of the cross-polarized induced current.

2. The Square Plate

The structure of dimensions 1 λ by 1 λ was divided in 64 monopoles, as shown in Figure 22. Eight current paths

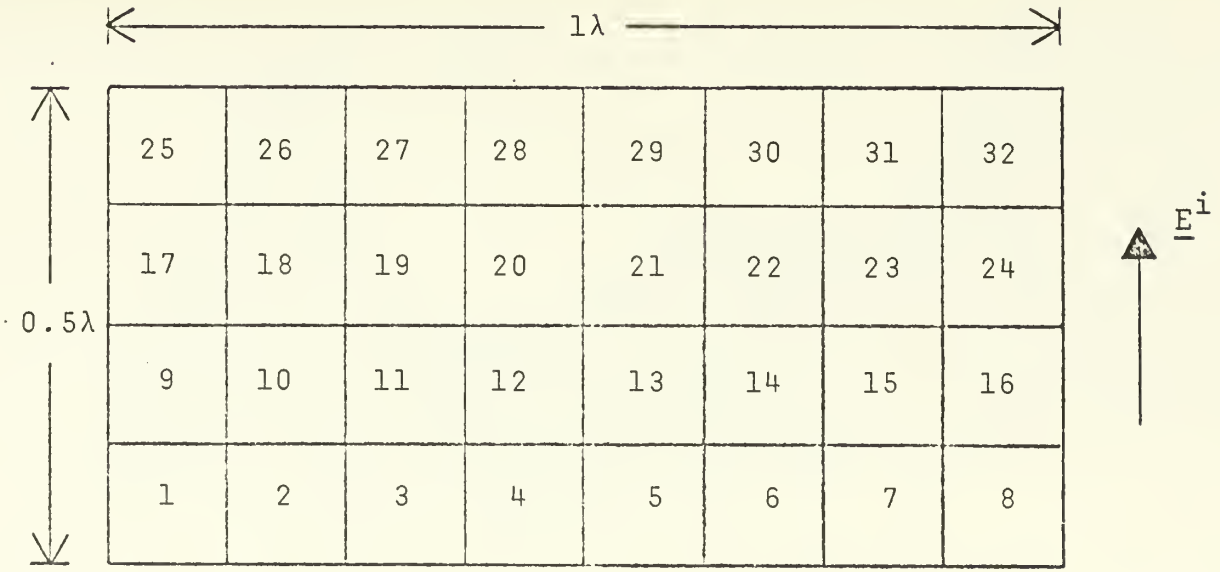

Figure 19. Rectangular Plate Segmented in 32 Monopoles. Plane Wave Incident at Broadside.

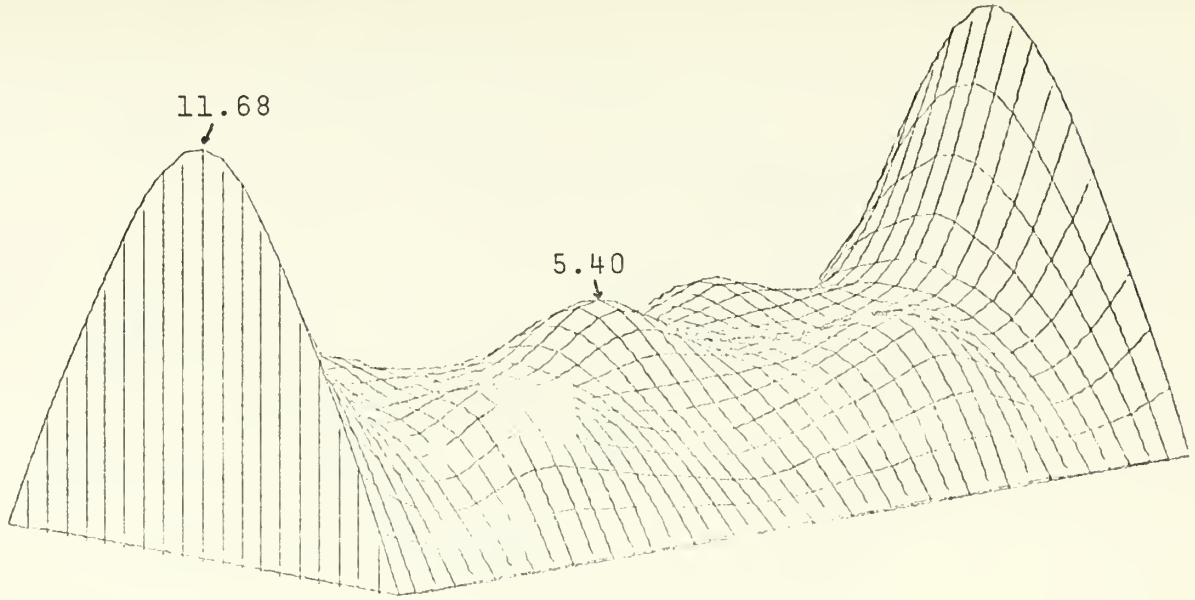

Figure 20. Rectangular Plate (1λ by 0.5λ) Current in the Direction of the Field.

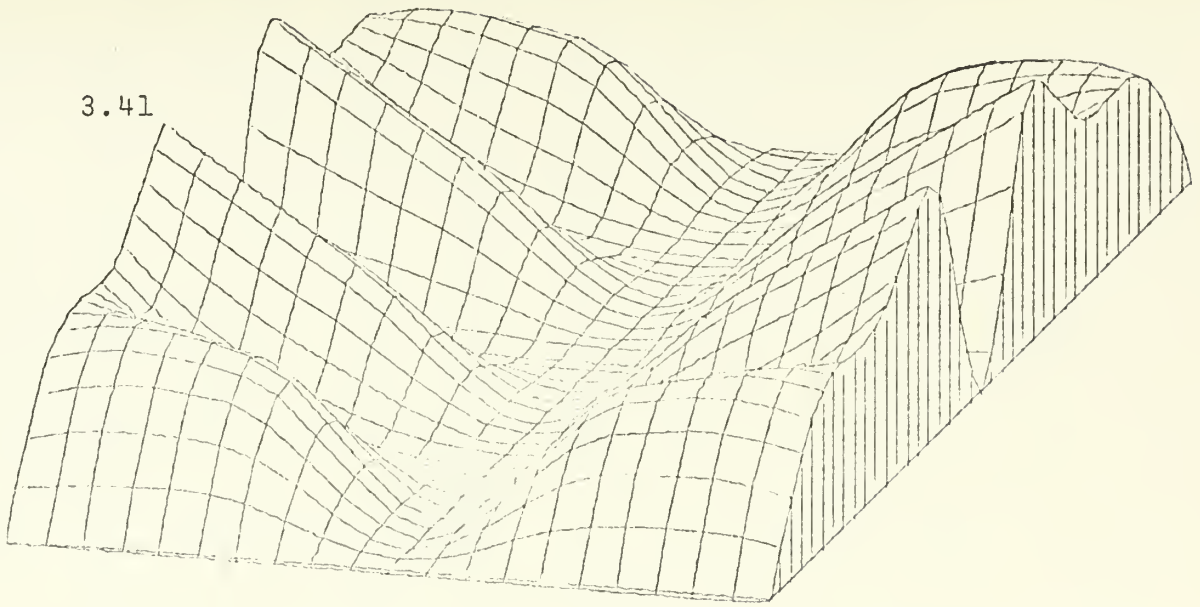

Figure 21. Rectangular Plate (1λ by 0.5λ) Cross-Polarized Current.

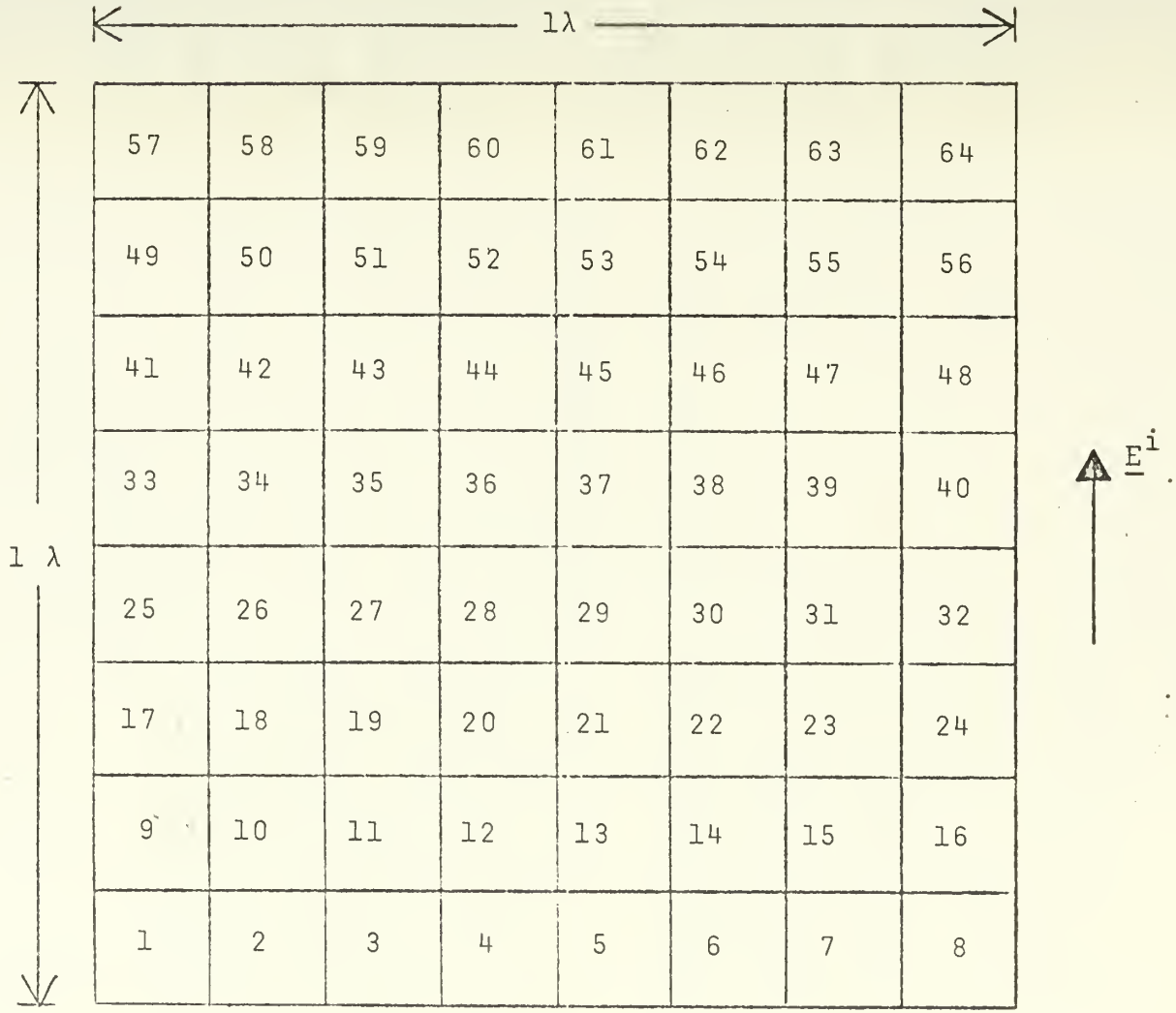

Figure 22. Square Plate Segmented in 64 Monopoles. Plane Wave Incident at Broadside.

were assumed in the z-direction and eight in the y-direction. Figure 23 shows the magnitude of the induced current in the direction of the field. Figure 24 shows the magnitude of the cross-polarized induced current.

3. The 'L'-Shaped Structure

The 'L'-shaped structure was divided in 48 monopoles as shown in Figure 25. The dimensions of the horizontal arm are 1 λ by 0.5 λ, and the vertical arm is 0.5 λ by 0.5 λ. Eight current paths were assumed in the z-direction and eight in the y-direction. Figure 26 shows the magnitude of the induced current in the direction of the field. Figure 27 shows the magnitude of the cross-polarized induced current.

4. The 'T'-Shaped Structure

The 'T'-shaped structure was divided in 48 monopoles as shown in Figure 28. The horizontal arm is 1 λ by 0.5 λ and the vertical arm is 0.5 λ by 0.5 λ. Eight current paths were assumed in the z-direction and eight in the y-direction. Figure 29 shows the magnitude of the induced current in the direction of the field. Figure 30 shows the magnitude of the cross-polarized induced current.

5. The Two-Dimensional Cross

The two-dimensional cross was divided in 48 monopoles as shown in Figure 31. The horizontal arm is 1 λ by 0.5 λ and the two vertical arms are 0.5 λ by 0.25 λ. Eight current path were assumed in the z-direction and eight in the y-direction. Figure 32 shows the magnitude of the current induced

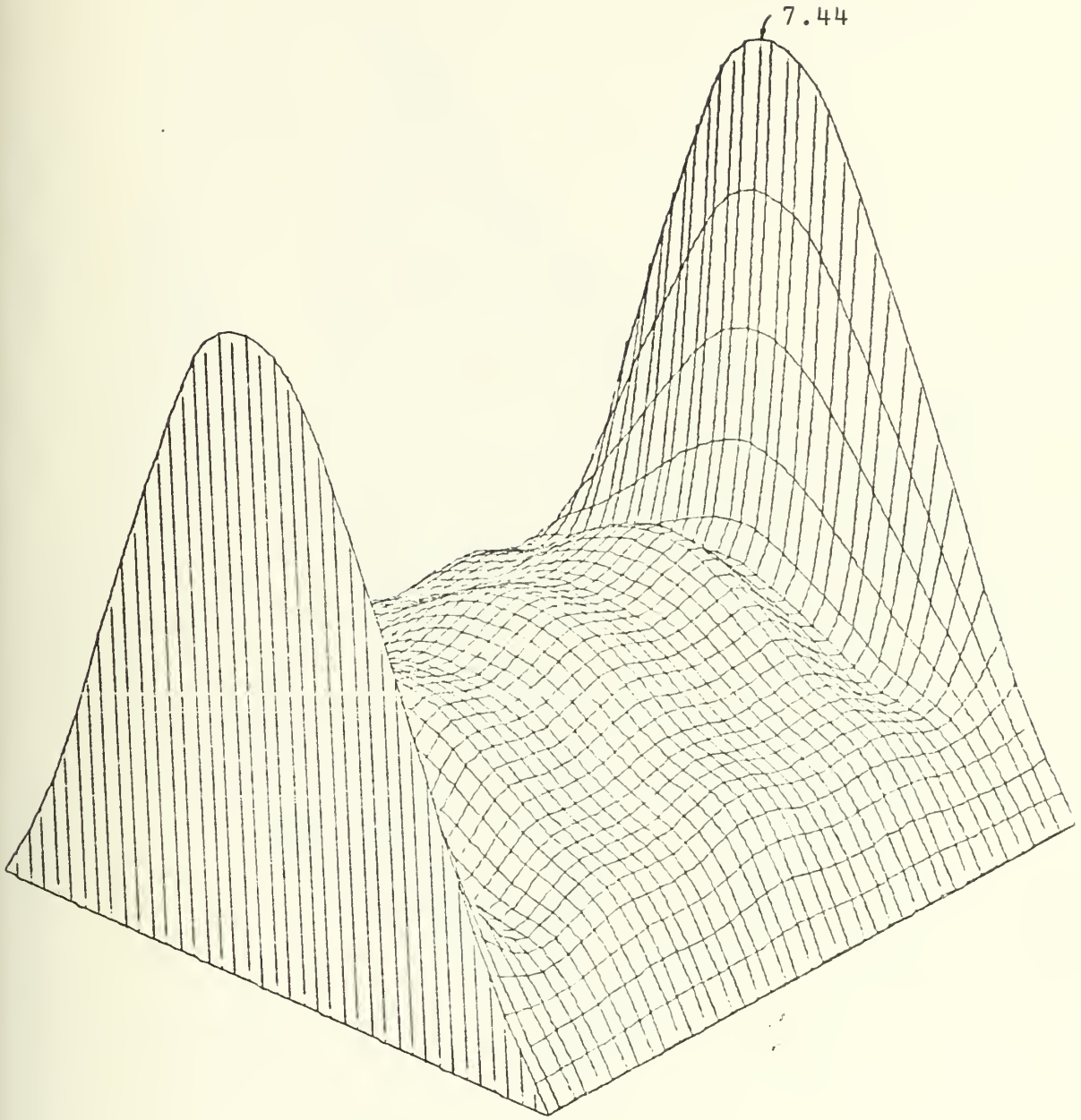

Figure 23. Square Plate (1 λ by 1 λ). Current in the Direction of the Field.

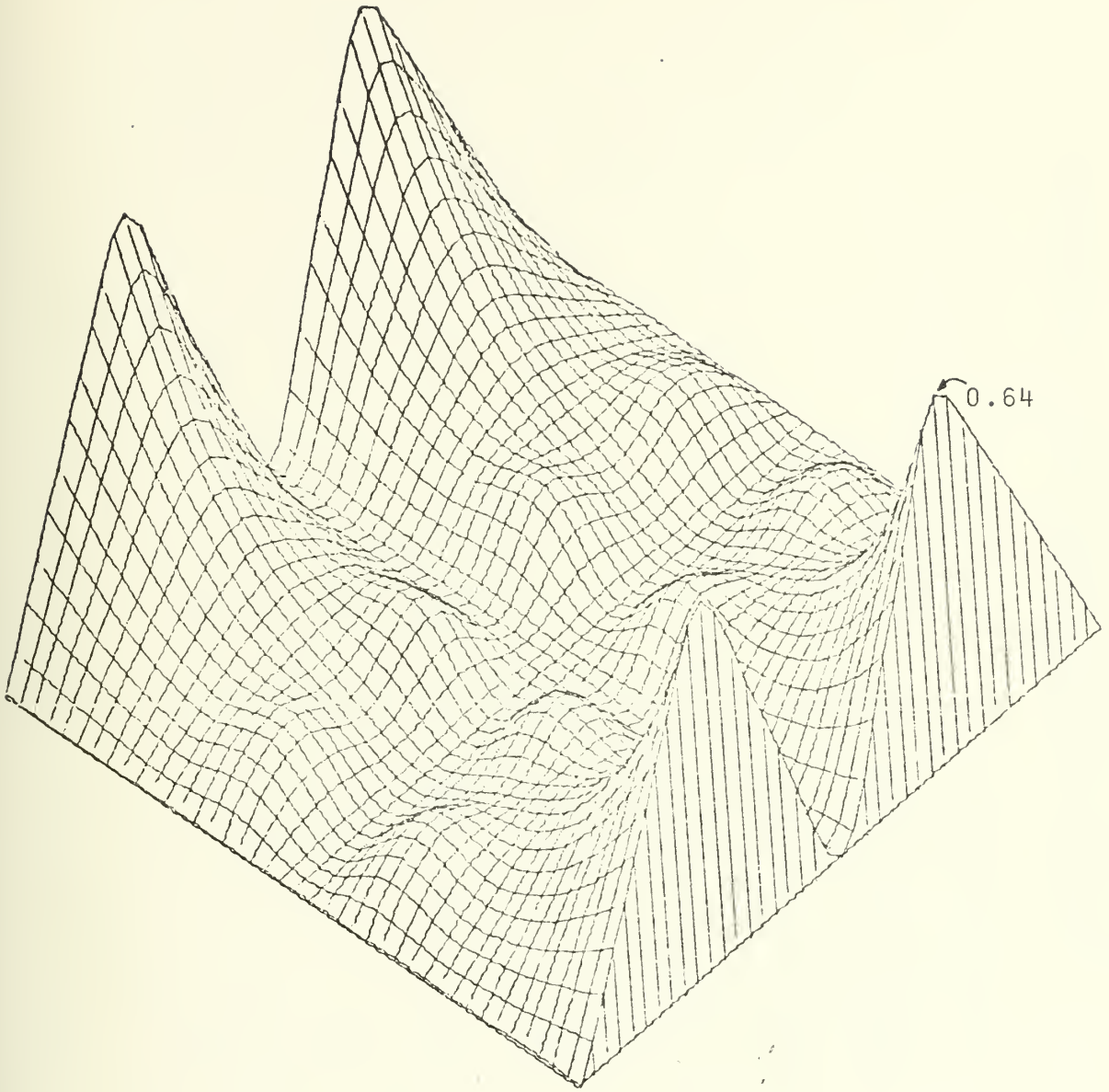

Figure 24. Square Plate (1 λ by 1 λ) Cross-Polarized Current.

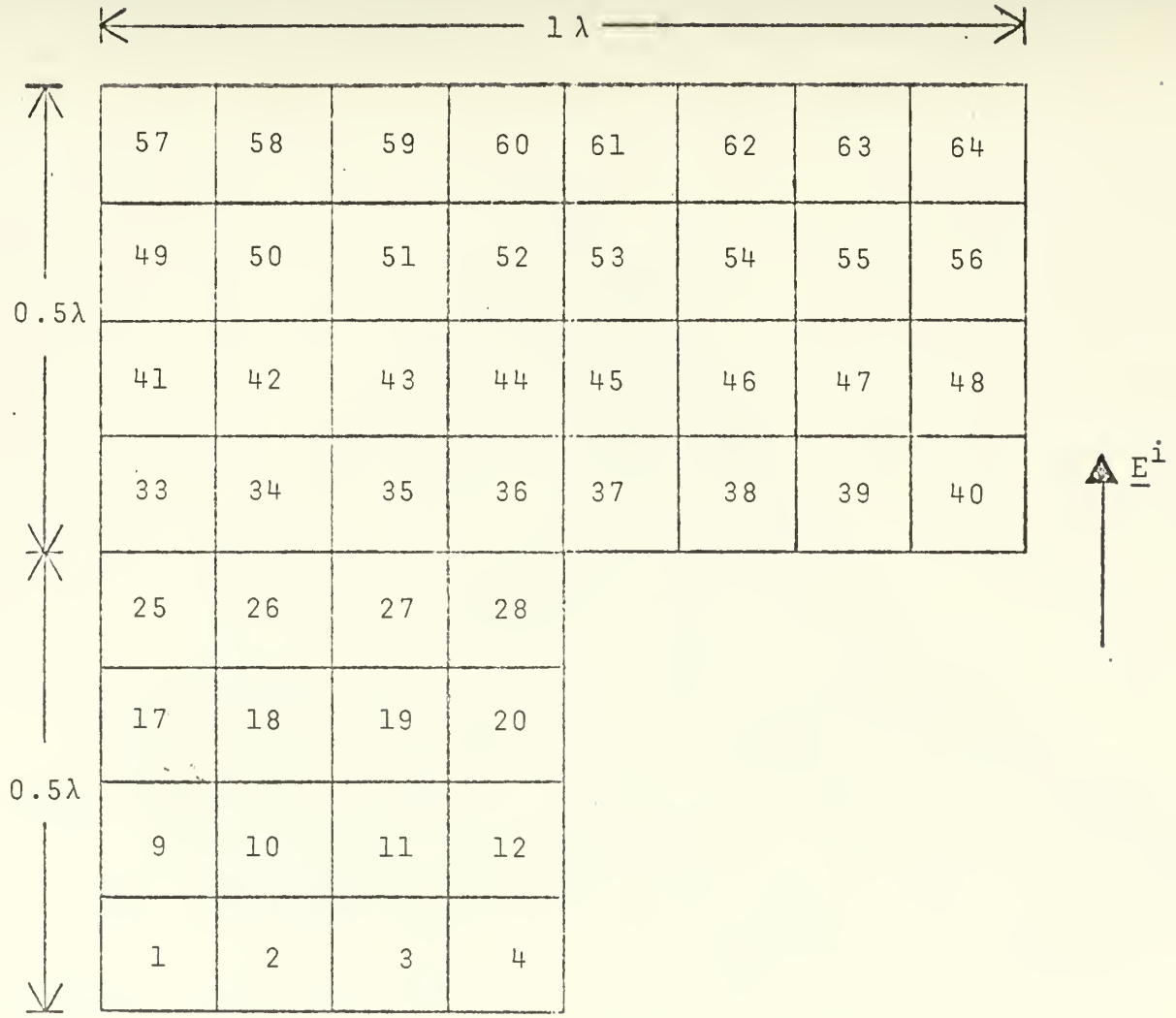

Figure 25. 'L'-Shaped Structure Segmented in 48 Monopoles. Plane Wave Incident at Broadside.

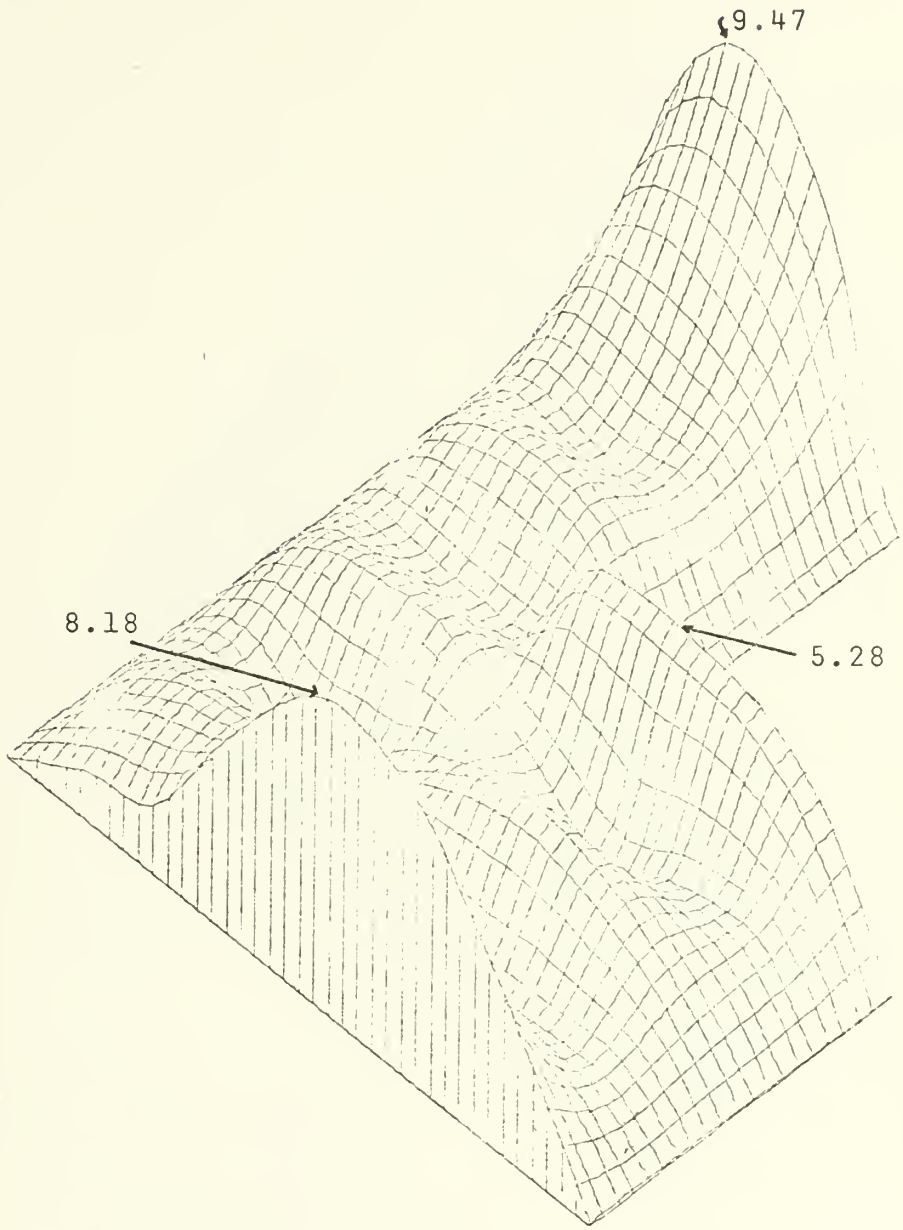

Figure 26. 'L'-Shaped Structure (1λ by 1λ) Current in the Direction of the Field.

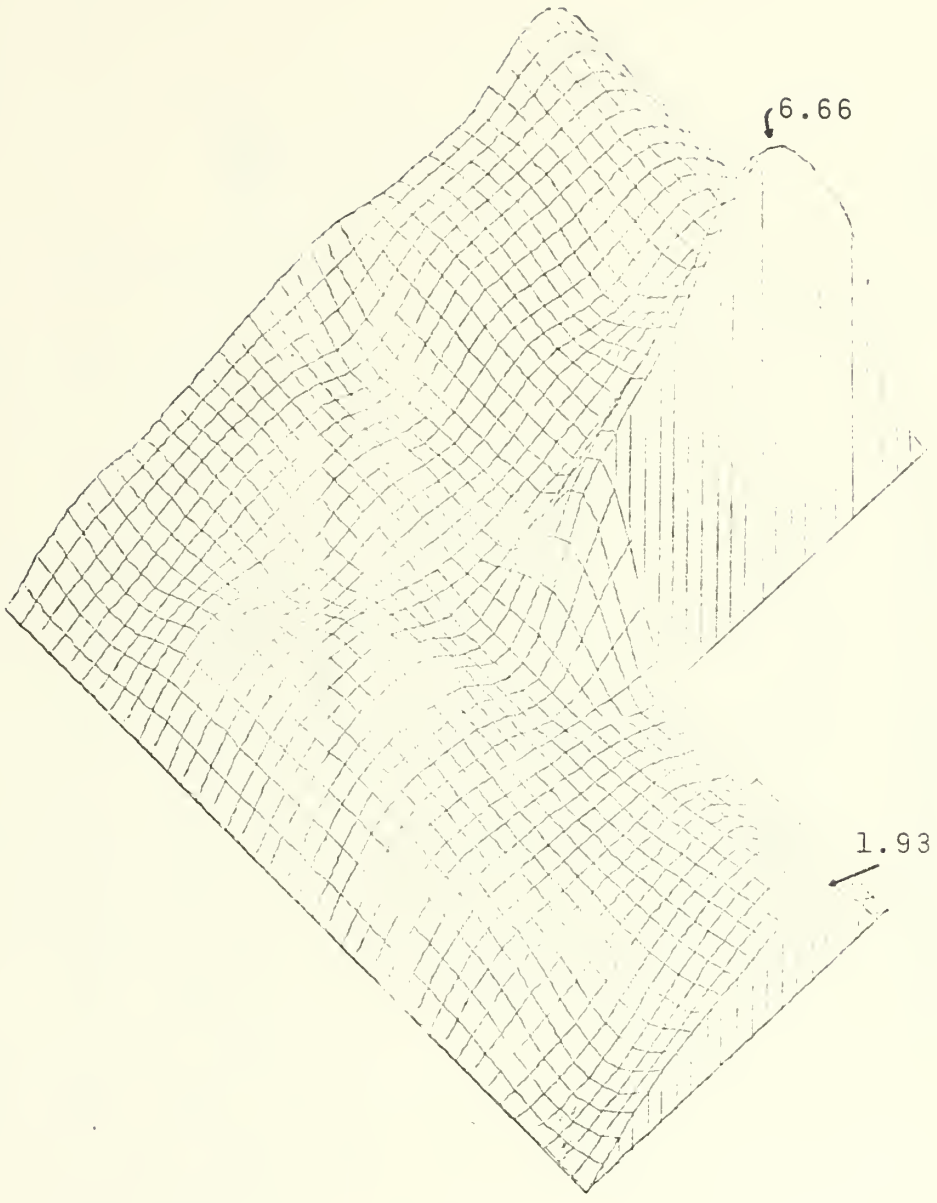

Figure 27. 'L'-Shaped Structure (1λ by 1λ) Cross-Polarized Current.

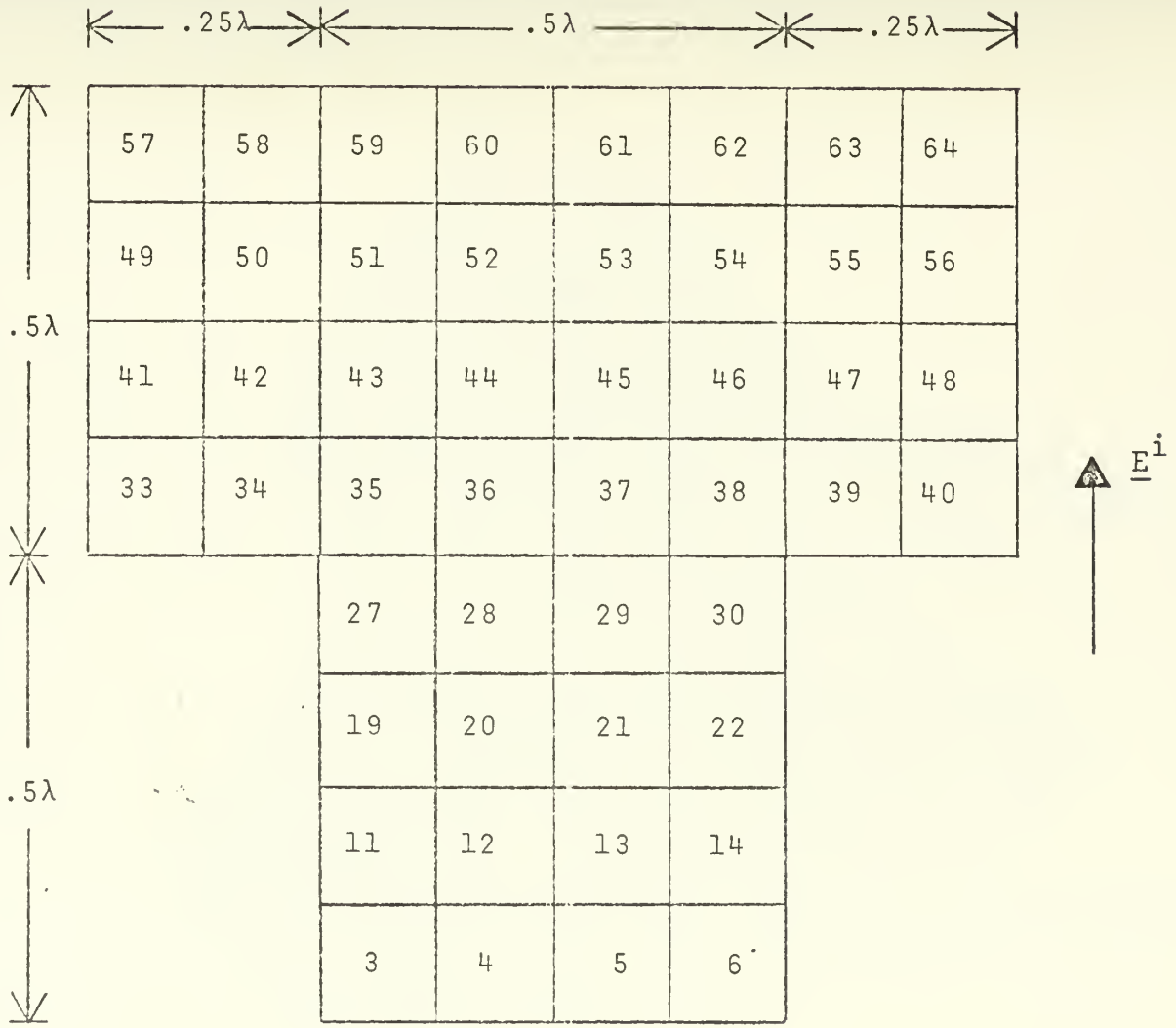

Figure 28. 'T'-Shaped Structure Segmented in 48 Monopoles. Plane Wave Incident at Broadside.

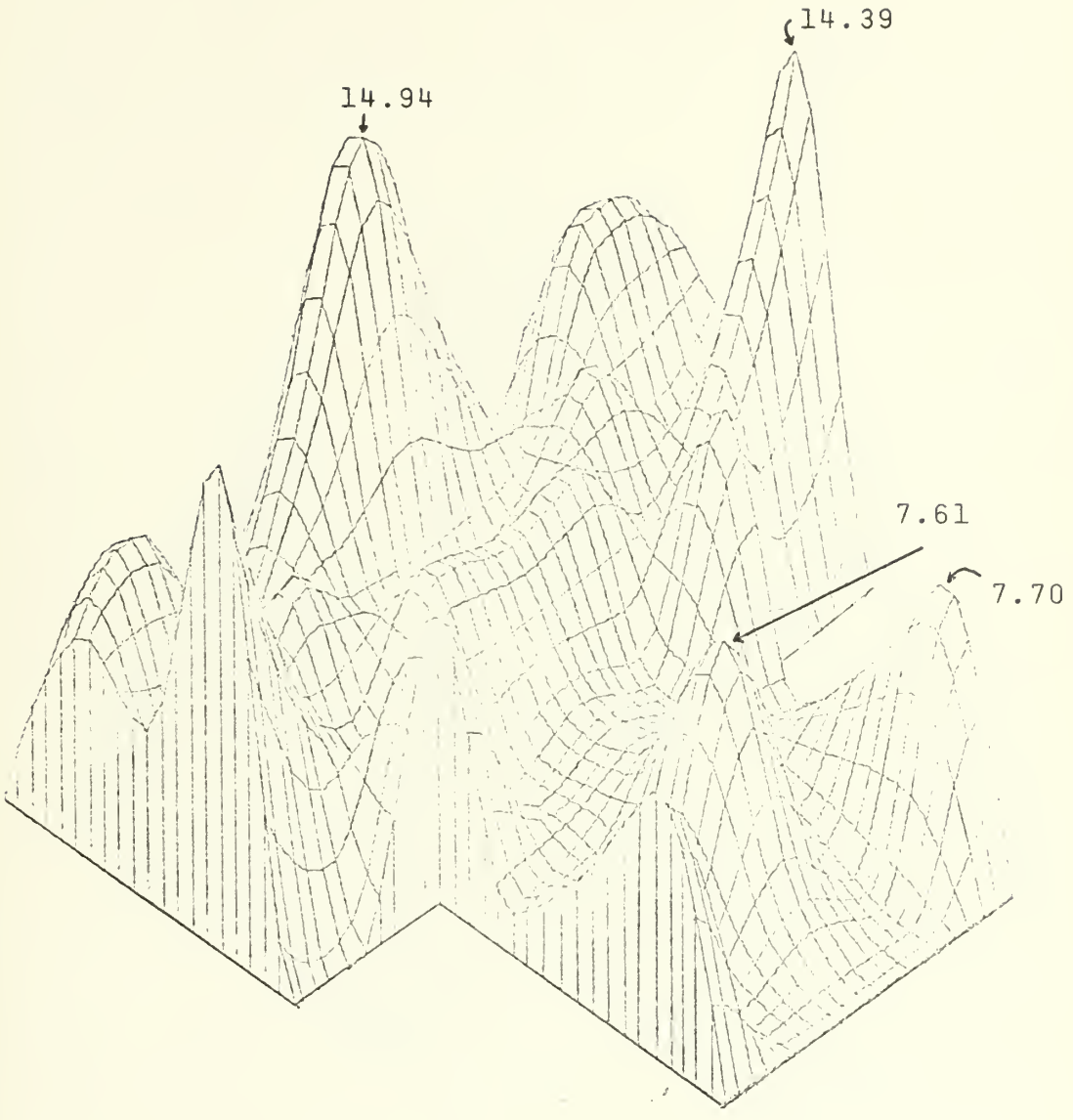

Figure 29. 'T'-Shaped Structure (1λ by 1λ) Current in the Direction of the Field.

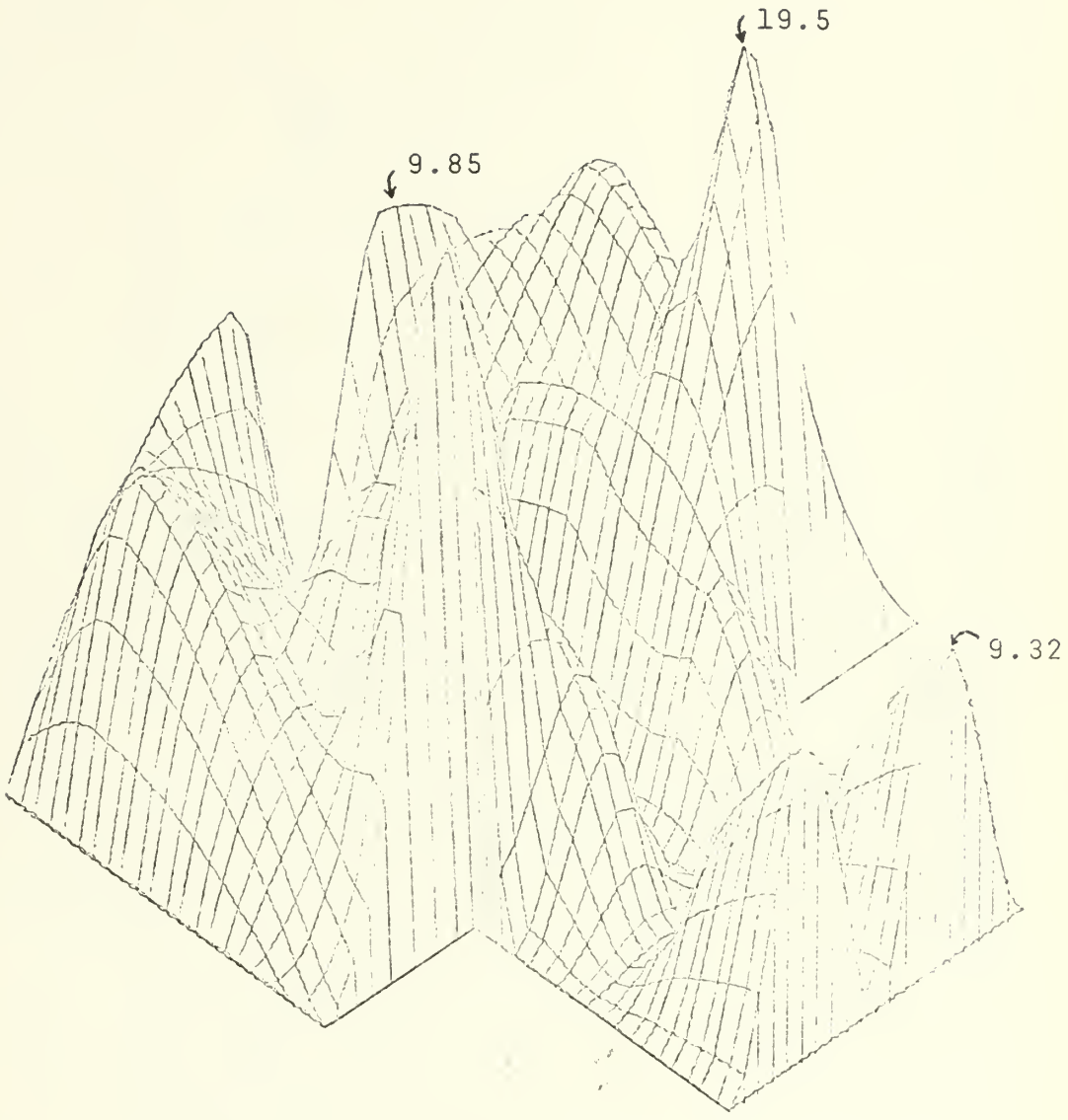

Figure 30. 'T'-Shaped Structure (1λ by 1λ) Cross-Polarized Current.

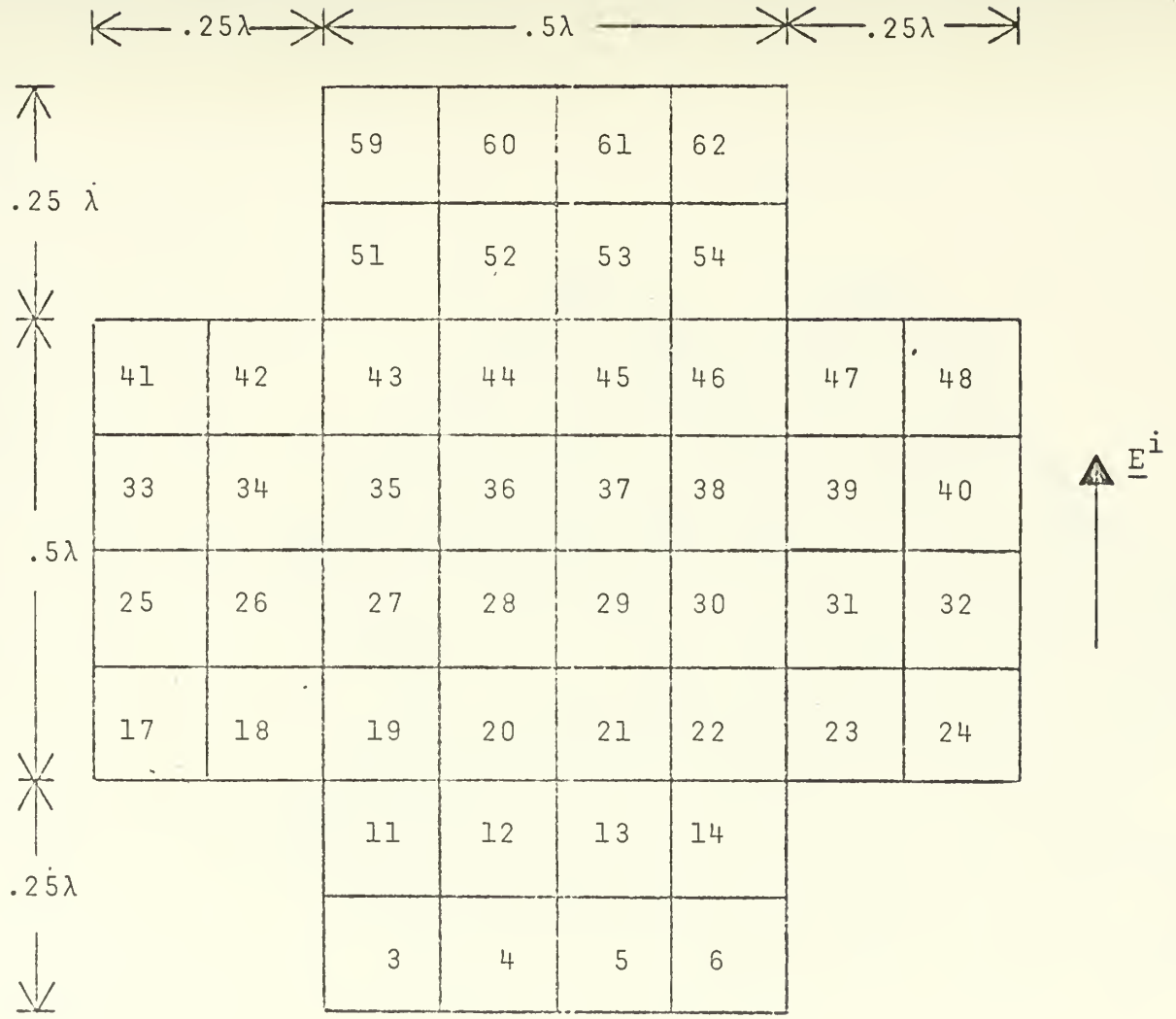

Figure 31. Two-Dimensional Cross Segmented in 48 Monompoles. Plane Wave Incdient at Broadside.

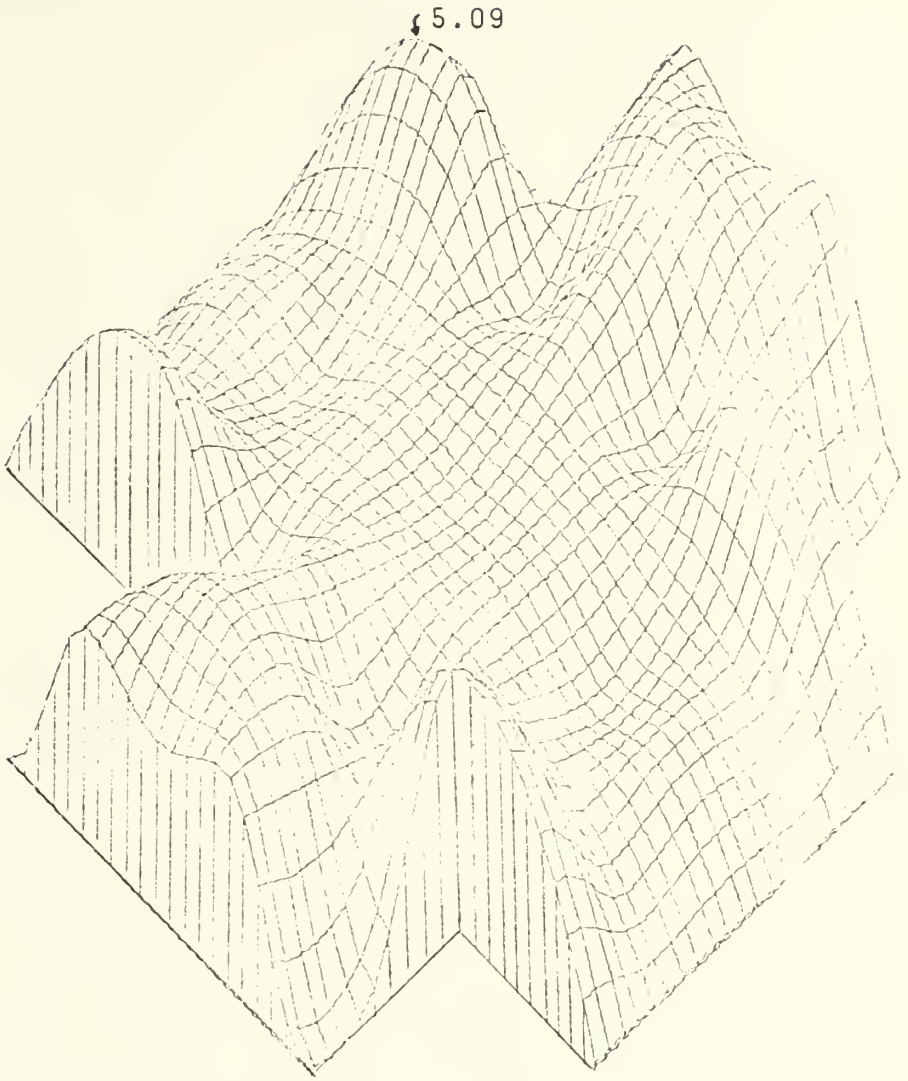

Figure 32. Two-Dimensional Cross (1λ by 1λ) Current in the Direction of the Field.

in the direction of the field. Figure 33 shows the magnitude of the cross-polarized induced current.

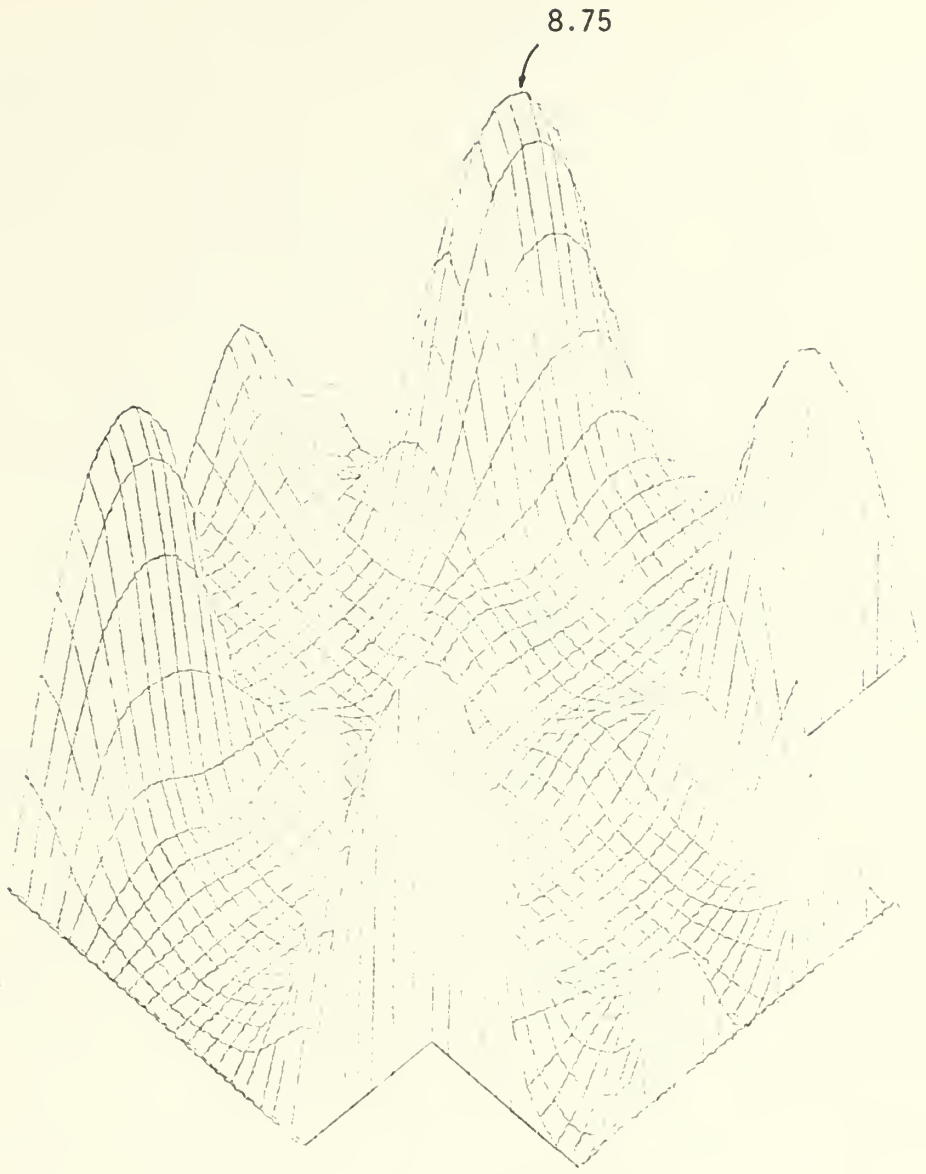

Figure 33. Two-Dimensional Cross (1λ by 1λ) Cross-Polarized Current.

IV. NUMERICAL RESULTS

The three-dimensional plots shown in the preceding section give a very good representation of the current density distribution over the two-dimensional structure. However, due to the fact that some of the points plotted come from interpolation and that the sub-program PL3TD1 is designed to plot only rectangular or squared surfaces, some accuracy is lost.

In the tables shown in this section, the exact values at the specific points are given.

For the Unidirectional Current Model the value of current is at the center of the dipole. For the General Current Method, the value of current is at the edges of the monopoles.

22.47	30.15	22.47
5.26	7.75	5.26
3.56	4.28	3.56
2.52	2.86	2.52
2.83	3.25	2.83
2.85	3.27	2.85
2.94	3.39	2.94
3.00	3.46	3.00
3.06	3.54	3.06
3.11	3.60	3.11
3.15	3.65	3.15
3.19	3.69	3.19
3.21	3.72	3.21
3.23	3.74	3.23
3.24	3.75	3.24
3.24	3.76	3.24
3.23	3.74	3.23
3.21	3.72	3.21
3.19	3.69	3.19
3.15	3.65	3.15
3.11	3.60	3.11
3.06	3.54	3.06
3.00	3.46	3.00
2.94	3.39	2.94
2.85	3.27	2.85
2.83	3.25	2.83
2.52	2.86	2.52
3.56	4.28	3.56
5.26	7.75	5.26
22.47	30.15	22.47

Table III. Rectangular Plate (Unidirectional Current Model) Magnitude of the Induced Current at the Center of the Dipole. See Figure 9.

4.38	8.56	4.38
1.43	2.57	1.43
1.57	2.73	1.57
1.47	2.38	1.47
1.50	2.32	1.50
1.53	2.30	1.53
1.58	2.32	1.58
1.62	2.36	1.62
1.67	2.40	1.67
1.70	2.45	1.70
1.74	2.49	1.74
1.77	2.53	1.77
1.79	2.56	1.79
1.80	2.58	1.80
1.81	2.59	1.81
1.81	2.59	1.81
1.80	2.58	1.80
1.79	2.56	1.79
1.76	2.53	1.76
1.74	2.49	1.74
1.70	2.45	1.70
1.67	2.40	1.67
1.62	2.36	1.62
1.58	2.32	1.58
1.53	2.30	1.53
1.49	2.32	1.49
1.47	2.38	1.47
1.57	2.73	1.57
1.43	2.57	1.43
4.38	8.56	4.38

Table IV. Square Plate (Unidirectional Current Model). Magnitude of the Induced Current at the Center of the Dipole. See Figure 11.

30.21		
7.22		
4.84		
3.07		
3.64		
3.64		
3.84		
3.99		
4.18		
4.37		
4.73		
4.89		
6.59		
5.76		
23.20		
41.16	3.73	29.67
11.60	2.45	9.51
2.50	2.48	3.27
2.53	2.46	1.33
1.51	2.45	1.47
1.79	2.44	1.39
1.66	2.41	1.47
1.63	2.40	1.49
1.57	2.37	1.50
1.52	2.36	1.49
1.46	2.39	1.49
1.45	2.46	1.47
1.50	2.82	1.61
1.51	2.66	1.35
3.97	8.75	4.77

Table V. 'L'-Shaped Structure (Unidirectional Circuit Model). Magnitude of the Induced Current at the Center of the Dipole. See Figure 13.

33.51		
7.56		
5.56		
3.60		
4.53		
6.15		
5.61		
24.17		
42.71	3.71	29.92
11.64	2.51	9.60
2.59	2.60	3.32
2.50	2.63	1.39
1.69	2.68	1.55
1.96	2.72	1.50
1.92	2.75	1.57
1.95	2.76	1.59
1.95	2.76	1.59
1.92	2.75	1.57
1.95	2.72	1.50
1.69	2.68	1.55
2.50	2.63	1.39
2.59	2.60	3.32
11.64	2.51	9.60
42.71	3.71	29.92
24.17		
5.61		
6.15		
4.53		
3.60		
5.56		
7.56		
33.51		

Table VI. 'T'-Shaped Structure (Unidirectional Current Model). Magnitude of the Induced Current at the Center of the Dipole. See Figure 15.

		12.8	16.7	12.8		
		3.16	4.20	3.16		
		4.05	4.78	4.05		
		9.30	12.2	9.30		
2.42	1.60	3.55	5.79	3.55	1.60	2.42
1.58	1.78	2.42	2.66	2.42	1.78	1.58
1.71	1.92	2.14	2.25	2.14	1.92	1.71
1.71	2.00	2.41	2.59	2.41	2.00	1.71
1.71	2.00	2.41	2.59	2.41	2.00	1.71
1.71	1.92	2.14	2.25	2.14	1.92	1.71
1.58	1.78	2.42	2.66	2.42	1.78	1.58
2.42	1.60	3.55	5.79	3.55	1.60	2.42
		9.30	12.2	9.30		
		4.05	4.78	4.05		
		3.16	4.20	3.16		
		12.8	16.7	12.8		

Table VII. Two-Dimensional Cross (Unidirectional Current Model). Magnitude of Induced Current at the Center of the Dipole. See Figure 17.

0.0	0.0	0.0	0.0	0.0	0.0	0.0	0.0	0.0
7.55	3.45	4.43	3.29	2.82	3.29	4.43	3.45	7.55
11.68	4.29	3.51	3.78	5.40	3.78	3.51	4.29	11.68
7.55	3.45	4.43	3.29	2.82	3.29	4.43	3.45	7.55
0.0	0.0	0.0	0.0	0.0	0.0	0.0	0.0	0.0

Table VIII. Rectangular Plate (General Current Model). Magnitude of Induced Current in the Direction of the Field. See Figure 19.

0.0	2.10	2.21	3.41	0.0	3.41	2.21	2.10	0.0
0.0	1.95	0.44	1.78	0.0	1.78	0.44	1.95	0.0
0.0	0.0	0.0	0.0	0.0	0.0	0.0	0.0	0.0
0.0	1.95	0.44	1.78	0.0	1.78	0.44	1.95	0.0
0.0	2.10	2.21	3.41	0.0	3.41	2.21	2.10	0.0

Table IX. Rectangular Plate (General Current Model). Magnitude of Cross-Polarized Induced Current. See Figure 19.

0.0	0.0	0.0	0.0	0.0	0.0	0.0	0.0	0.0
1.73	1.14	1.41	1.38	1.61	1.38	1.41	1.14	1.73
4.23	1.33	1.81	1.77	1.95	1.77	1.81	1.33	4.23
6.53	1.75	2.42	2.29	2.52	2.29	2.42	1.75	6.53
7.44	2.04	2.70	2.44	2.74	2.44	2.70	2.04	7.44
6.53	1.75	2.42	2.29	2.52	2.29	2.42	1.75	6.53
4.23	1.33	1.81	1.77	1.95	1.77	1.81	1.33	4.23
1.73	1.14	1.41	1.38	1.61	1.38	1.41	1.14	1.73
0.0	0.0	0.0	0.0	0.0	0.0	0.0	0.0	0.0

Table X. Square Plate (General Current Model). Magnitude of Induced Current in the Direction of the Field. See Figure 22.

0.0	0.32	0.64	0.37	0.0	0.37	0.64	0.32	0.0
0.0	0.16	0.30	0.17	0.0	0.17	0.30	0.16	0.0
0.0	0.08	0.14	0.10	0.0	0.10	0.14	0.08	0.0
0.0	0.11	0.06	0.13	0.0	0.13	0.06	0.11	0.0
0.0	0.0	0.0	0.0	0.0	0.0	0.0	0.0	0.0
0.0	0.11	0.06	0.13	0.0	0.13	0.06	0.11	0.0
0.0	0.08	0.14	0.10	0.0	0.10	0.14	0.08	0.0
0.0	0.16	0.30	0.17	0.0	0.17	0.30	0.16	0.0
0.0	0.32	0.64	0.37	0.0	0.37	0.64	0.32	0.0

Table XI. Square Plate (General Current Model). Magnitude of Cross-Polarized Induced Current. See Figure 22.

0.0	0.0	0.0	0.0	0.0	0.0	0.0	0.0	0.0
1.15	2.08	1.53	2.55	2.03	2.84	2.43	4.28	7.60
1.80	2.86	0.38	3.29	1.77	3.65	2.09	4.40	9.47
5.14	2.81	1.34	3.25	1.86	3.19	2.50	3.47	6.92
7.79	1.74	2.77	1.99	5.13	0.0	0.0	0.0	0.0
8.18	0.85	3.68	0.62	5.28				
6.60	1.07	3.36	1.49	5.04				
3.55	1.25	2.22	1.99	3.71				
0.0	0.0	0.0	0.0	0.0				

Table XII. 'L'-Shaped Structure (General Current Model). Magnitude of Induced Current in the Direction of the Field. See Figure 25.

0.0	1.03	1.06	1.43	1.75	1.43	1.31	2.16	0.0
0.0	0.57	1.07	1.16	0.54	1.73	1.56	1.52	0.0
0.0	1.29	0.67	1.05	0.66	1.25	0.84	1.25	0.0
0.0	1.44	1.41	0.68	0.76	1.23	2.07	1.41	0.0
0.0	1.56	1.42	0.57	3.44	4.78	6.66	4.87	0.0
0.0	1.32	1.06	0.63	0.0				
0.0	0.95	0.93	0.91	0.0				
0.0	0.13	1.04	1.38	0.0				
0.0	1.09	1.58	1.93	0.0				

Table XIII. 'L'-Shaped Structure (General Current Model). Magnitude of Cross Polarized Induced Current. See Figure 25.

0.0	0.0	0.0	0.0	0.0	0.0	0.0	0.0	0.0
6.22	7.74	1.73	7.58	14.94	7.58	1.72	7.74	6.22
5.03	2.80	6.49	3.68	2.69	3.68	6.49	2.80	5.03
14.39	6.45	2.94	6.47	5.81	6.47	2.94	6.45	14.39
0.0	0.0	8.32	1.73	2.68	1.73	8.32	0.0	0.0
		1.07	1.81	3.13	1.81	1.07		
		3.74	1.05	7.61	1.05	3.74		
		7.70	0.07	1.33	0.07	7.70		
		0.0	0.0	0.0	0.0	0.0		

Table XIV. 'T'-Shaped Structure (General Current Model). Magnitude of Induced Current in the Direction of the Field. See Figure 28.

0.0	4.95	8.21	9.86	0.0	9.85	8.21	4.95	0.0
0.0	9.63	5.69	2.57	0.0	2.57	5.69	9.63	0.0
0.0	7.75	1.69	7.88	0.0	7.88	1.69	7.75	0.0
0.0	4.33	5.45	8.90	0.0	8.90	5.45	4.33	0.0
0.0	1.30	19.50	8.58	0.0	8.58	19.50	1.30	0.0
		0.0	5.85	0.0	5.85	0.0		
		0.0	0.49	0.0	0.49	0.0		
		0.0	5.84	0.0	5.84	0.0		
		0.0	9.32	0.0	9.32	0.0		

Table XV. 'T'-Shaped Structure (General Current Model). Magnitude of Cross-Polarized Induced Current. See Figure 28.

		0.0	0.0	0.0	0.0	0.0		
		4.15	1.70	2.03	1.70	4.15		
0.0	0.0	5.09	2.45	1.60	2.45	5.09	0.0	0.0
4.29	3.74	1.92	2.75	2.73	2.75	1.92	3.74	4.29
3.45	5.01	4.08	3.13	2.58	3.13	4.08	5.01	3.45
4.29	3.74	1.92	2.75	2.74	2.75	1.92	3.74	4.29
0.0	0.0	5.09	2.45	1.60	2.45	5.09	0.0	0.0
		4.15	1.70	2.03	1.70	4.15		
		0.0	0.0	0.0	0.0	0.0		

Table XVI. Two-Dimensional Cross (General Current Model). Magnitude of Induced Current in the Direction of the Field. See Figure 31.

		0.0	3.23	0.0	3.23	0.0		
		0.0	0.68	0.0	0.68	0.0		
0.0	8.75	8.27	0.34	0.0	0.34	8.27	8.75	0.0
0.0	1.21	0.42	1.12	0.0	1.12	0.42	1.21	0.0
0.0	0.0	0.0	0.0	0.0	0.0	0.0	0.0	0.0
0.0	1.21	0.42	1.12	0.0	1.12	0.42	1.21	0.0
0.0	8.75	8.27	0.34	0.0	0.34	8.27	8.75	0.0
		0.0	0.68	0.0	0.68	0.0		
		0.0	3.23	0.0	3.23	0.0		

Table XVII. Two-Dimensional Cross (General Current Model). Magnitude of Cross-Polarized Induced Current. See Figure 31.

V. CONCLUSIONS AND RECOMMENDATIONS

The results shown for the rectangular plate (Unidirectional Current Model) has been compared with those presented by Richmond and Wang [Ref. 3]. The results shown for the square plate (General Current Model) has been compared with those presented by Rahmat-Samii and Mittra [Ref. 4]. Both comparisons are seen to be in good agreement.

A comparison of the results for the Unidirectional Current Model and the General Current Model for similar geometries, suggest that a solution for the current distribution in two-dimensional structures is not complete if the cross-polarized current is neglected. This problem is more remarkable where the junction problem is present, such as in the 'L', 'T' and cross shaped structures. In these structures the magnitude of the cross-polarized current reaches values of the same order of magnitude as that for the current in the direction of the field, and in some cases as for the 'T'-shaped structure and the two-dimensional cross the maximum values found for the cross-polarized current are somewhat larger than those of the current in the direction of the field.

The computer programs used in the General Current Model do not fully apply symmetry in the calculation of the coupling between dipoles. Since this calculation is the predominant in computer time consumption, some improvements should be investigated in order to be able to solve more

complicated geometries without the restriction of "computer time."

A program of surface current measurement for flat-plate structures with corner notches, similar to the 'T', 'L' and cross structures, should be valuable for validating these and other computer codes for two-dimensional surfaces.

APPENDIX A: FORTRAN PROGRAM LISTING

```
      COMPUTER PROGRAM 1
C
      REAL LAMDA(30),A(30),RANGE(4),JSAB(90),JSPH(90),JSRE(90),JSIM(90),
     1K
      COMPLEX C(90,90),X(90),R(90),ZSDPAR,JS(90)
C
C     L1=MAXIMUM NUMBER OF DIPOLES IN A ROW
C     L3=NUMBER OF ROWS OF DIPOLES
C     L7=TOTAL NUMBER OF DIPOLES
C
C     INITIALIZATION
      L1=30
      L2=L1-1
      L3=3
      L7=90
      L8=L3-1
      L9=L1
      D=1./4.
      W=1./30.
      DO 1 M=1,L7
      A(M)=0.0
      X(M)=(0.0,0.0)
      R(M)=(0.0,0.0)
      JSAB(M)=0.0
      JSPH(M)=0.0
      JSRE(M)=0.0
      JSIM(M)=0.0
      JS(M)=(0.0,0.0)
      DO 2 N=1,L7
      C(M,N)=(0.0,0.0)
    2 CONTINUE
    1 CONTINUE
      DO 3 M=1,L1
      LAMDA(M)=0.0
    3 CONTINUE
      NY=4
      NYP=5
      XC=0.0
      L=1
C
C     END OF INITIALIZATION
C
      WRITE (6,90)
   90 FORMAT('1',23X,'M',2X,'N',14X,'C(M,N)'/)
C
```

```
C       100 LOOP TO CHANGE THE POSITION OF THE Z-AXIS
C
        DO 100 IH=1,L3
        LL2=L+L2
C
C       200 LOOP TO CHANGE THE POSITION OF THE Y-AXIS
C
        DO 200 M=L,LL2
        ZO=IH*D
        J=1
C
C       300 LOOP TO CHANGE THE Z-COORDINATE OF THE SOURCE DIPOLE
C
        DO 300 IK=1,L3
C
C       M IS THE TOTAL NUMBER OF DIPOLES
C       I IS THE NUMBER OF DIPOLES IN A ROW
C       THIS STEP IS TO AVOID I GREATER THAN L1
C
        IF(M.LE.L1)I=M
        IF(M.LE.L1)GO TO 390
        DO 350 MITO=1,L8
        I=M-(MITO*L1)
        IF((I.GT.0).AND.(I.LE.L1))GO TO 390
  350 CONTINUE
  390 CONTINUE
        ZO=ZO-D
        YO=-(I*W)
        JL2=J+L2
C
C       400 LOOP TO CHANGE THE Y-COORDINATE OF THE SOURCE DIPOLE
C
        DO 400 N=J,JL2
        YO=YO+W
C
C
C       AVOID THE BUNCH OF IF STATEMENTS FOR THE FIRST REFERENCE DIPOLE
C
        IF(M.EQ.1)GO TO 490
C
C
C       BUNCH OF IF STATEMENTS TO AVOID UNNECESSARY CALCULATION OF THE
C       COUPLING TERM BY APPLYING SYMMETRY
C
        IFLAG=IABS(IK-IH)
        IF (IFLAG.NE.0) GO TO 460
        DO 450 IFLOOP=1,L1
        ITEST=IFLOOP-1
```

```
      IF (IABS(M-N).EQ.ITEST) C(M,N)=C(1,IFLOOP)
  450 CONTINUE
      GO TO 510
  460 DO 466 IFLOOP=1,L1
      IFMAX=(IFLAG*L1)-1+IFLOOP
      IFMIN=(IFLAG*L1)+1-IFLOOP
      LP=(IFLAG*L1)+IFLOOP
      IF ((IABS(M-N).EQ.IFMAX).OR.(IABS(M-N).EQ.IFMIN)) C(M,N)=C(1,LP)
  466 CONTINUE
      GO TO 510
C
C     END OF IF STATEMENTS (SYMMETRY)
C
C
C     CALCULATE THE COUPLING TERM
C
  490 C(M,N)=ZSDPAR(D,W,XO,YO,ZO,NY,NYP)
  510 CONTINUE
C
C     N IS THE TOTAL NUMBER OF DIPOLES.THIS STATEMENT(S) ASURES THAT THE
C     LIMITS OF DO 400 WILL VARY BETWEEN THE NUMBER ASSIGNED TO THE
C     DIPOLES IN THE WINGS OF THE ROW
C
      IF(N.EQ.JL2)J=N+1
  400 CONTINUE
  300 CONTINUE
  200 CONTINUE
C
C     THIS STATEMENNT(S) ASURES THAT THE LIMITS OF DO 200 WILL VARY
C     BETWEEN THE NUMBER ASSIGNED TO THE DIPOLES IN THE WINGS OF THE ROW
C
      IF(L8.EQ.0)GO TO 570
      DO 570 IM=1,L8
      IF(M.EQ.(IM*L1))L=(IM*L1)+1
  570 CONTINUE
  100 CONTINUE
C
      DO 591 M=1,L7,5
      DO 592 N=1,L7,5
      WRITE(6,500)M,N,C(M,N)
  500 FORMAT (' ',20X,2I4,4X,2F12.5)
  592 CONTINUE
  591 CONTINUE
C
      WRITE (6,600)
  600 FORMAT ('1','    ')
      PI=3.141592654
      K=2*PI
```

```
C
C       CALCULATE THE RIGHT HAND SIDE VECTOR (SELF REACTION TERM)
C
        WRITE (6,700)
  700 FORMAT ('0','RIGHT HAND SIDE VECTOR (SELF REACTION) ')
        AR=((2*W)/(K*SIN(K*D)))*(1-COS(K*D))
        DO 1000 M=1,L7
        A(M)=AR
        WRITE (6,900)M,A(M)
  900 FORMAT (' ',' A(',I3,')=',F12.5)
 1000 CONTINUE
C
C       INVERT THE COEFFICIENT MATRIX
C
        CALL CMTRIN (L7,C,L7,DETERM)
C
        WRITE (6,2300)
 2300 FORMAT ('1',' ')
C
C       CALCULATE THE VALUE OF THE SAMPLE VECTOR
C
        WRITE (6,2350)
 2350 FORMAT ('0','THE SAMPLE VECTOR AT EACH SURFACE DIPOLE IS')
        DO 2400 M=1,L7
        X(M)=( 0.0, 0.0)
        DO 2500 N=1,L7
        R(N)=C(M,N)*A(N)
        X(M)=X(M)+R(N)
 2500 CONTINUE
        WRITE (6,2600)M,X(M)
 2600 FORMAT (' ','X(',I3,')=',2X,E14.7,2X,E14.7)
 2400 CONTINUE
        WRITE (6,2700)
 2700 FORMAT ('1','   ')
C
C
C       CALCULATE THE VALUE OF THE SURFACE CURRENT (JS), ITS ABSOUTE VALUE
C       (JSAB) AND ITS PHASE (JSPH).
C
        DO 3000 M=1,L7
        JS(M)=X(M)*(120.*PI)/(W**2)
        JSAB(M)=CABS(JS(M))
        JSRE(M)=REAL(JS(M))
        JSIM(M)=AIMAG(JS(M))
        JSPH(M)=(ATAN(JSIM(M)/JSRE(M)))*360/(2*PI)
        IF(JSPH(M).LT.0.0)JSPH(M)=JSPH(M)+360.
 3000 CONTINUE
        END
```

```
      COMPUTER PROGRAM 2
C
      REAL LAMDA(30),A(60),RANGE(4),JSAB(60),JSPH(60),JSRE(60),JSIM(60),
     1K
      COMPLEX C(90,90),CX(60,60),X(60),R(60),ZSDPAR,JS(60)
C
CC
C     L1=MAXIMUM NUMBER OF DIPOLES IN A ROW
C     L2=L1-1
C     L3=NUMBER OF ROWS OF DIPOLES
C     L7=TOTAL NUMBER OF EFFECTIVE DIPOLES
C     L8=L3-1
C     L9=NUMBER OF SOLUTION POINTS
C     L10=MINIMUM NUMBER OF DIPOLES IN A ROW
C     L11=L10-1
C     L12=FIRST DIPOLE IN A ''LITTLE'' ROW
C     L13=LARGE DIPOLE IN A LARGE ROW
C     L14=L12+L10
C     L15=TOTAL NUMBER OF DIPOLES (REAL + FICTICIOUS)
C     L16=LAST COMMON DIPOLE TO REAL AND FICTICIOUS
C     L17=L1*2
C     L18=L16+1
C     L19=L16+L10
C     L20=L17-L16
CC
CC
C     INITIALIZATION
C
      L1=30
      L2=29
      L3=3
      L7=60
      L8=2
      L9=30
      L10=15
      L11=14
      L12=31
      L13=30
      L14=46
      L15=90
      L16=45
      L17=60
      L18=46
      L19=60
      L20=15
      D=1./4.
      W=1./30.
      DO 1 M=1,L7
```

```
      A(M)=0.0
      X(M)=(0.0,0.0)
      R(M)=(0.0,0.0)
      DO 2 N=1,L7
      CX(M,N)=(0.0,0.0)
    2 CONTINUE
    1 CONTINUE
      DO 3 M=1,L7
      LAMDA(M)=0.0
      JSAB(M)=0.0
      JSPH(M)=0.0
      JSRE(M)=0.0
      JSIM(M)=0.0
      JS(M)=(0.0,0.0)
    3 CONTINUE
      DO 4 M=1,L15
      DO 5 N=1,L15
      C(M,N)=(0.0,0.0)
    5 CONTINUE
    4 CONTINUE
      NY=4
      NYP=5
      XO=0.0
      L=1
C
CC    END OF INITIALIZATION
CC
C     WRITE (6,90)
   90 FORMAT('1',23X,'M',2X,'N',14X,'C(M,N)'/)
C
CC    100 LOOP TO CHANGE THE POSITION OF THE Z-AXIS
C
      DO 100 IH=1,L3
      LL2=L+L2
C
CC    200 LOOP TO CHANGE THE POSITION OF THE Y-AXIS
C
      DO 200 M=L,LL2
      ZO=IH*D
      J=1
C
CC    300 LOOP TO CHANGE THE Z-COORDINATE OF THE SOURCE DIPOLE
C
      DO 300 IK=1,L3
C
CC    M IS THE TOTAL NUMBER OF DIPOLES
CC    I IS THE NUMBER OF DIPOLES IN A ROW
C     THIS STEP IS TO AVOID I GREATER THAN L1
```

```
C
      IF(M.LE.L1)I=M
      IF(M.LE.L1)GO TO 390
      DO 350 MITO=1,L8
      I=M-(MITO*L1)
      IF((I.GT.0).AND.(I.LE.L1))GO TO 390
  350 CONTINUE
  390 CONTINUE
      ZO=ZO-D
      YO=-(I*W)
      JL2=J+L2
C
CC    400 LOOP TO CHANGE THE Y-COORDINATE OF THE SOURCE DIPOLE
C
      DO 400 N=J,JL2
      YO=YO+W
C
CC    AVOID THE BUNCH OF IF STATEMENTS FOR THE FIRST REFERENCE DIPOLE
C
      IF(M.EQ.1)GO TO 490
C
CC    BUNCH OF IF STATEMENTS TO AVOID UNNECESSARY CALCULATION OF THE
CC    COUPLING TERM BY APPLYING SYMMETRY
C
C
      IFLAG=IABS(IK-IH)
      IF (IFLAG.NE.0) GO TO 460
      DO 450 IFLOOP=1,L1
      ITEST=IFLOOP-1
      IF (IABS(M-N).EQ.ITEST) C(M,N)=C(1,IFLOOP)
  450 CONTINUE
      GO TO 510
  460 DO 466 IFLOOP=1,L1
      IFMAX=(IFLAG*L1)-1+IFLOOP
      IFMIN=(IFLAG*L1)+1-IFLOOP
      LP=(IFLAG*L1)+IFLOOP
      IF ((IABS(M-N).EQ.IFMAX).OR.(IABS(M-N).EQ.IFMIN)) C(M,N)=C(1,LP)
  466 CONTINUE
      GO TO 510
C
CC    END OF IF STATEMENTS (SYMMETRY)
C
CC    CALCULATE THE COUPLING TERM
C
  490 C(M,N)=ZSDPAR(D,W,XO,YO,ZO,NY,NYP)
  510 CONTINUE
C
C     N IS THE TOTAL NUMBER OF DIPOLES.THIS STATEMENT(S) ASURES THAT THE
```

```
C      LIMITS OF DO 400 WILL VARY BETWEEN THE NUMBER ASSIGNED TO THE
C      DIPOLES IN THE WINGS OF THE ROW
C
       IF(N.EQ.JL2)J=N+1
  400  CONTINUE
  300  CONTINUE
  200  CONTINUE
C
C      THIS STATEMENNT(S) ASURES THAT THE LIMITS OF DO 200 WILL VARY
C      BETWEEN THE NUMBER ASSIGNED TO THE DIPOLES IN THE WINGS OF THE ROW
C
       DO 570 IM=1,L8
       IF(M.EQ.(IM*L1))L=(IM*L1)+1
  570  CONTINUE
  100  CONTINUE
C
C      THIS STATEMENTS ASURES THAT THE COUPLING C(M,N) IS CORRECTLY
C      ASSIGNED TO THE PROPER TERM OF THE CX(M,N) MATRIX
C
       DO 501 M=1,L7
       IF((M.GE.  1).AND.(M.LE.L16))IND1=M
       IF((M.GE.L18).AND.(M.LE.L19))IND1=M+L20
       DO 502 N=1,L16
       IND2=N
       CX(M,N)=C(IND1,IND2)
  502  CONTINUE
       DO 503 N=L18,L19
       IND2=N+L20
       CX(M,N)=C(IND1,IND2)
  503  CONTINUE
  501  CONTINUE
C
       DO 591 M=1,L7,5
       DO 592 N=1,L7,5
       WRITE(6,500)M,N,CX(M,N)
  500  FORMAT (' ',20X,2I4,4X,2F12.5)
  592  CONTINUE
  591  CONTINUE
       WRITE (6,593)
  593  FORMAT('1','   ')
       DO 594 M=1,L15,5
       DO 595 N=1,L15,5
       WRITE (6,500)M,N,C(M,N)
  595  CONTINUE
  594  CONTINUE
C
       WRITE (6,600)
  600  FORMAT ('1','    ')
```

```
      PI=3.141592654
      K=2*PI
C
C     CALCULATE THE RIGHT HAND SIDE VECTOR (SELF REACTION TERM)
C
      WRITE (6,700)
  700 FORMAT ('0','RIGHT HAND SIDE VECTOR (SELF REACTION) ')
      AR=((2*W)/(K*SIN(K*D)))*(1-COS(K*D))
      DO 1000 M=1,L7
      A(M)=AR
      WRITE (6,900)M,A(M)
  900 FORMAT (' ',' A(',I3,')=',F12.5)
 1000 CONTINUE
C
C     INVERT THE COEFFICIENT MATRIX
C
      CALL CMTRIN (L7,CX,L7,DETERM)
      WRITE (6,2300)
 2300 FORMAT ('1','  ')
C
C     CALCULATE THE VALUE OF THE SAMPLE VECTOR
C
      WRITE (6,2350)
 2350 FORMAT ('0','THE SAMPLE VECTOR AT EACH SURFACE DIPOLE IS')
      DO 2400 M=1,L7
      X(M)=( 0.0, 0.0)
      DO 2500 N=1,L7
      R(N)=CX(M,N)*A(N)
      X(M)=X(M)+R(N)
 2500 CONTINUE
      WRITE (6,2600)M,X(M)
 2600 FORMAT (' ','X(',I3,')=',2X,E14.7,2X,E14.7)
 2400 CONTINUE
      WRITE (6,2700)
 2700 FORMAT ('1','   ')
C
C     CALCULATE THE VALUE OF THE SURFACE CURRENT (JS), ITS ABSOLUTE
C     VALUE (JSAB) AND ITS PHASE (JSPH)
C
      DO 3000 M=1,L7
      JS(M)=X(M)*(120.*PI)/(W**2)
      JSAB(M)=CABS(JS(M))
      JSRE(M)=REAL(JS(M))
      JSIM(M)=AIMAG(JS(M))
      JSPH(M)=(ATAN(JSIM(M)/JSRE(M)))*360/(2*PI)
      IF(JSPH(M).LT.0.0)JSPH(M)=JSPH(M)+360.
 3000 CONTINUE
      END
```

```
      COMPUTER PROGRAM 3
C
      REAL LAMDA(32),A(64),RANGE(4),JSAB(64),JSPH(64),JSRE(64),JSIM(64),
     1MAGN(32),PHASE(32),K
      COMPLEX C(96,96),CX(64,64),X(64),R(64),ZSDPAR,JS(64)
C
CC
CC    L1=MAXIMUM NUMBER OF DIPOLES IN A ROW
CC    L2=L1-1
CC    L3=NUMBER OF ROWS OF DIPOLES
CC    L7=TOTAL NUMBER OF EFFECTIVE DIPOLES
CC    L8=L3-1
CC    L9=NUMBER OF SOLUTION POINTS
CC    L10=MINIMUM NUMBER OF DIPOLES IN A ROW
CC    L15=TOTAL NUMBER OF DIPOLES (REAL + FICTICIOUS)
CCC
CCC   INITIALIZATION
C
      L1=32
      L2=31
      L3=3
      L7=64
      L8=2
      L9=32
      L10=16
      L15=96
      D=1./4.
      W=1./32.
      DO 1 M=1,L7
      A(M)=0.0
      X(M)=(0.0,0.0)
      R(M)=(0.0,0.0)
      JSAB(M)=0.0
      JSPH(M)=0.0
      JSRE(M)=0.0
      JSIM(M)=0.0
      JS(M)=(0.0,0.0)
      DO 2 N=1,L7
      CX(M,N)=(0.0,0.0)
    2 CONTINUE
    1 CONTINUE
      DO 3 M=1,L7
      LAMDA(M)=0.0
    3 CONTINUE
      DO 4 M=1,L15
      DO 5 N=1,L15
      C(M,N)=(0.0,0.0)
```

```
    5 CONTINUE
    4 CONTINUE
      NY=4
      NYP=5
      XO=0.0
      L=1
C
C     END OF INITIALIZATION
C
      WRITE (6,90)
   90 FORMAT('1',23X,'M',2X,'N',14X,'C(M,N)'/)
C
C     100 LOOP TO CHANGE THE POSITION OF THE Z-AXIS
C
      DO 100 IH=1,L3
      LL2=L+L2
C
C     200 LOOP TO CHANGE THE POSITION OF THE Y-AXIS
C
      DO 200 M=L,LL2
      ZO=IH*D
      J=1
C
C     300 LOOP TO CHANGE THE Z-COORDINATE OF THE SOURCE DIPOLE
C
      DO 300 IK=1,L3
C
C     M IS THE TOTAL NUMBER OF DIPOLES
C     I IS THE NUMBER OF DIPOLES IN A ROW
C     THIS STEP IS TO AVOID I GREATER THAN L1
C
      IF(M.LE.L1)I=M
      IF(M.LE.L1)GO TO 390
      DO 350 MITO=1,L8
      I=M-(MITO*L1)
      IF((I.GT.0).AND.(I.LE.L1))GO TO 390
  350 CONTINUE
  390 CONTINUE
      ZO=ZO-D
      YO=-(I*W)
      JL2=J+L2
C
C     400 LOOP TO CHANGE THE Y-COORDINATE OF THE SOURCE DIPOLE
C
      DO 400 N=J,JL2
      YO=YO+W
C
C     AVOID THE BUNCH OF IF STATEMENTS FOR THE FIRST REFERENCE DIPOLE
```

```
C
      IF(M.EQ.1)GO TO 490
C
C     BUNCH OF IF STATEMENTS TO AVOID UNNECESSARY CALCULATION OF THE
C     COUPLING TERM BY APPLYING SYMMETRY
C
      IFLAG=IABS(IK-IH)
      IF (IFLAG.NE.0) GO TO 460
      DO 450 IFLOOP=1,L1
      ITEST=IFLOOP-1
      IF (IABS(M-N).EQ.ITEST) C(M,N)=C(1,IFLOOP)
  450 CONTINUE
      GO TO 510
  460 DO 466 IFLOOP=1,L1
      IFMAX=(IFLAG*L1)-1+IFLOOP
      IFMIN=(IFLAG*L1)+1-IFLOOP
      LP=(IFLAG*L1)+IFLOOP
      IF ((IABS(M-N).EQ.IFMAX).OR.(IABS(M-N).EQ.IFMIN)) C(M,N)=C(1,LP)
  466 CONTINUE
      GO TO 510
C
C     END OF IF STATEMENTS (SYMMETRY)
C
C     CALCULATE THE COUPLING TERM
C
  490 C(M,N)=ZSDPAR(D,W,XO,YO,ZO,NY,NYP)
  510 CONTINUE
C
C     N IS THE TOTAL NUMBER OF DIPOLES.THIS STATEMENT(S) ASURES THAT THE
C     LIMITS OF DO 400 WILL VARY BETWEEN THE NUMBER ASSIGNED TO THE
C     DIPOLES IN THE WINGS OF THE ROW
C
      IF(N.EQ.JL2)J=N+1
  400 CONTINUE
  300 CONTINUE
  200 CONTINUE
C
C     THIS STATEMENNT(S) ASURES THAT THE LIMITS OF DO 200 WILL VARY
C     BETWEEN THE NUMBER ASSIGNED TO THE DIPOLES IN THE WINGS OF THE ROW
C
      DO 570 IM=1,L8
      IF(M.EQ.(IM*L1))L=(IM*L1)+1
  570 CONTINUE
  100 CONTINUE
C
C     THIS STATEMENTS ASURES THAT THE COUPLING C(M,N) IS CORRECTLY
C     ASSIGNED TO THE PROPER TERM OF THE CX(M,N) MATRIX
C
```

```
      DO 501 M=1,64
      IF((M.GE. 1).AND.(M.LE.32)) IND1=M
      IF((M.GE.33).AND.(M.LE.48)) IND1=M+8
      IF((M.GE.49).AND.(M.LE.64)) IND1=M+24
      DO 502 N=1,32
      IND2=N
      CX(M,N)=C(IND1,IND2)
  502 CONTINUE
      DO 503 N=33,48
      IND2=N+8
      CX(M,N)=C(IND1,IND2)
  503 CONTINUE
      DO 504 N=49,64
      IND2=N+24
      CX(M,N)=C(IND1,IND2)
  504 CONTINUE
  501 CONTINUE
C
      DO 591 M=1,L7,5
      DO 592 N=1,L7,5
      WRITE(6,500)M,N,CX(M,N)
  500 FORMAT (' ',20X,2I4,4X,2F12.5)
  592 CONTINUE
  591 CONTINUE
      WRITE (6,593)
  593 FORMAT('1',' ')
      DO 594 M=1,L15,5
      DO 595 N=1,L15,5
      WRITE (6,500)M,N,C(M,N)
  595 CONTINUE
  594 CONTINUE
      WRITE (6,600)
  600 FORMAT ('1',' ')
      PI=3.141592654
      K=2*PI
C
C     CALCULATE THE RIGHT HAND SIDE VECTOR (SELF REACTION TERM)
C
      WRITE (6,700)
  700 FORMAT ('0','RIGHT HAND SIDE VECTOR (SELF REACTION) ')
      AR=((2*W)/(K*SIN(K*D)))*(1-COS(K*D))
      DO 1000 M=1,L7
      A(M)=AR
      WRITE (6,900)M,A(M)
  900 FORMAT (' ',' A(',I3,')=',F12.5)
 1000 CONTINUE
C
C     INVERT THE COEFFICIENT MATRIX
```

```
C
      CALL CMTRIN (L7,CX,L7,DETERM)
      WRITE (6,2300)
 2300 FORMAT ('1','  ')
C
C     CALCULATE THE VALUE OF THE SAMPLE VECTOR
C
      WRITE (6,2350)
 2350 FORMAT ('0','THE SAMPLE VECTOR AT EACH SURFACE DIPOLE IS')
      DO 2400 M=1,L7
      X(M)=( 0.0, 0.0)
      DO 2500 N=1,L7
      R(N)=CX(M,N)*A(N)
      X(M)=X(M)+R(N)
 2500 CONTINUE
      WRITE (6,2600)M,X(M)
 2600 FORMAT (' ','X(',I3,')=',2X,E14.7,2X,E14.7)
 2400 CONTINUE
      WRITE (6,2700)
 2700 FORMAT ('1','   ')
C
C     CALCULATE THE VALUE OF THE SURFACE CURRENT (JS), ITS ABSOLUTE
C     VALUE (JSAB) AND ITS PHASE (JSPH)
C
      DO 3000 M=1,L7
      JS(M)=X(M)*(120.*PI)/(W**2)
      JSAB(M)=CABS(JS(M))
      JSRE(M)=REAL(JS(M))
      JSIM(M)=AIMAG(JS(M))
      JSPH(M)=(ATAN(JSIM(M)/JSRE(M)))*360/(2*PI)
      IF(JSPH(M).LT.0.0)JSPH(M)=JSPH(M)+360.
 3000 CONTINUE
      END
```

```
      COMPUTER PROGRAM 4
C
CC
      REAL LAMDA(16),A(80),RANGE(4),JSAB(80),JSPH(80),JSRE(80),JSIM(80),
     1K
      COMPLEX C(112,112),CX(80,80),X(80),R(80),ZSDPAR,JS(80)
C
CCC
CCC   L1=MAXIMUM NUMBER OF DIPOLES IN A ROW
CCC   L2=L1-1
CCC   L3=NUMBER OF ROWS OF DIPOLES
CCC   L7=TOTAL NUMBER OF EFFECTIVE DIPOLES
CCC   L8=L3-1
CCC   L9=NUMBER OF SOLUTION POINTS
CCC   L10=MINIMUM NUMBER OF DIPOLES IN A ROW
CCC   L15=TOTAL NUMBER OF DIPOLES (REAL + FICTICIOUS)
CCCCC
CCCCC INITIALIZATION
CC
      L1=16
      L2=L1-1
      L3=7
      L7=80
      L8=L3-1
      L9=16
      L10=8
      L15=112
      D=1./8.
      W=1./16.
C
CC
      DO 1 M=1,L7
      A(M)=0.0
      X(M)=(0.0,0.0)
      R(M)=(0.0,0.0)
      JSAB(M)=0.0
      JSPH(M)=0.0
      JSRE(M)=0.0
      JSIM(M)=0.0
      JS(M)=(0.0,0.0)
      DO 2 N=1,L7
      CX(M,N)=(0.0,0.0)
    2 CONTINUE
    1 CONTINUE
      DO 3 M=1,L7
      LAMDA(M)=0.0
    3 CONTINUE
```

```
      DO 4 M=1,L15
      DO 5 N=1,L15
      C(M,N)=(0.0,0.0)
    5 CONTINUE
    4 CONTINUE
      NY=4
      NYP=5
      XO=0.0
      L=1
C
C     END OF INITIALIZATION
C
      WRITE (6,90)
   90 FORMAT('1',23X,'M',2X,'N',14X,'C(M,N)'/)
C
C     100 LOOP TO CHANGE THE POSITION OF THE Z-AXIS
C
      DO 100 IH=1,L3
      LL2=L+L2
C
C     200 LOOP TO CHANGE THE POSITION OF THE Y-AXIS
C
      DO 200 M=L,LL2
      ZO=IH*D
      J=1
C
C     300 LOOP TO CHANGE THE Z-COORDINATE OF THE SOURCE DIPOLE
C
      DO 300 IK=1,L3
C
C     M IS THE TOTAL NUMBER OF DIPOLES
C     I IS THE NUMBER OF DIPOLES IN A ROW
C     THIS STEP IS TO AVOID I GREATER THAN L1
C
      IF(M.LE.L1)I=M
      IF(M.LE.L1)GO TO 390
      DO 350 MITO=1,L8
      I=M-(MITO*L1)
      IF((I.GT.0).AND.(I.LE.L1))GO TO 390
  350 CONTINUE
  390 CONTINUE
      ZO=ZO-D
      YO=-(I*W)
      JL2=J+L2
C
C     400 LOOP TO CHANGE THE Y-COORDINATE OF THE SOURCE DIPOLE
C
      DO 400 N=J,JL2
```

```
      YO=YO+W
C
CC    AVOID THE BUNCH OF IF STATEMENTS FOR THE FIRST REFERENCE DIPOLE
C
      IF(M.EQ.1)GO TO 490
C
CC
CC    BUNCH OF IF STATEMENTS TO AVOID UNNECESSARY CALCULATION OF THE
CC    COUPLING TERM BY APPLYING SYMMETRY
C
      IFLAG=IABS(IK-IH)
      IF (IFLAG.NE.0) GO TO 460
      DO 450 IFLOOP=1,L1
      ITEST=IFLOOP-1
      IF (IABS(M-N).EQ.ITEST) C(M,N)=C(1,IFLOOP)
  450 CONTINUE
      GO TO 510
  460 DO 466 IFLOOP=1,L1
      IFMAX=(IFLAG*L1)-1+IFLOOP
      IFMIN=(IFLAG*L1)+1-IFLOOP
      LP=(IFLAG*L1)+IFLOOP
      IF ((IABS(M-N).EQ.IFMAX).OR.(IABS(M-N).EQ.IFMIN)) C(M,N)=C(1,LP)
  466 CONTINUE
      GO TO 510
C
CC    END OF IF STATEMENTS (SYMMETRY)
CC
CC    CALCULATE THE COUPLING TERM
C
  490 C(M,N)=ZSDPAR(D,W,XO,YO,ZO,NY,NYP)
  510 CONTINUE
C
CC    N IS THE TOTAL NUMBER OF DIPOLES.THIS STATEMENT(S) ASURES THAT THE
CC    LIMITS OF DO 400 WILL VARY BETWEEN THE NUMBER ASSIGNED TO THE
CC    DIPOLES IN THE WINGS OF THE ROW
C
      IF(N.EQ.JL2)J=N+1
  400 CONTINUE
  300 CONTINUE
  200 CONTINUE
C
CC    THIS STATEMENNT(S) ASURES THAT THE LIMITS OF DO 200 WILL VARY
CC    BETWEEN THE NUMBER ASSIGNED TO THE DIPOLES IN THE WINGS OF THE ROW
C
      DO 570 IM=1,L8
      IF(M.EQ.(IM*L1))L=(IM*L1)+1
  570 CONTINUE
  100 CONTINUE
```

```
C
CC      THIS STATEMENTS ASURES THAT THE COUPLING C(M,N) IS CORRECTLY
CC      ASSIGNED TO THE PROPER TERM OF THE CX(M,N) MATRIX
C
        DO 501 M=1,L7
        IF((M.GE. 1).AND.(M.LE. 8)) IND1=M+ 4
        IF((M.GE. 9).AND.(M.LE.16)) IND1=M+ 12
        IF((M.GE.17).AND.(M.LE.64)) IND1=M+ 16
        IF((M.GE.65).AND.(M.LE.72)) IND1=M+ 20
        IF((M.GE.73).AND.(M.LE.80)) IND1=M+ 28
        DO 502 N=1,8
        IND2=N+4
        CX(M,N)=C(IND1,IND2)
  502 CONTINUE
        DO 503 N=9,16
        IND2=N+12
        CX(M,N)=C(IND1,IND2)
  503 CONTINUE
        DO 504 N=17,64
        IND2=N+16
        CX(M,N)=C(IND1,IND2)
  504 CONTINUE
        DO 506 N=65,72
        IND2=N+20
        CX(M,N)=C(IND1,IND2)
  506 CONTINUE
        DO 507 N=73,80
        IND2=N+28
        CX(M,N)=C(IND1,IND2)
  507 CONTINUE
  501 CONTINUE
        DO 591 M=1,L7,5
        DO 592 N=1,L7,5
        WRITE(6,500)M,N,CX(M,N)
  500 FORMAT (' ',20X,2I4,4X,2F12.5)
  592 CONTINUE
  591 CONTINUE
        WRITE (6,593)
  593 FORMAT('1','   ')
        DO 594 M=1,L15,5
        DO 595 N=1,L15,5
        WRITE (6,500)M,N,C(M,N)
  595 CONTINUE
  594 CONTINUE
C
        WRITE (6,600)
  600 FORMAT ('1','    ')
        PI=3.141592654
```

```
      K=2*PI
C
C     CALCULATE THE RIGHT HAND SIDE VECTOR (SELF REACTION TERM)
C
      WRITE (6,700)
  700 FORMAT ('0','RIGHT HAND SIDE VECTOR (SELF REACTION) ')
      AR=((2*W)/(K*SIN(K*D)))*(1-COS(K*D))
      DO 1000 M=1,L7
      A(M)=AR
      WRITE (6,900)M,A(M)
  900 FORMAT (' ',' A(',I3,')=',F12.5)
 1000 CONTINUE
C
C     INVERT THE COEFFICIENT MATRIX
C
      CALL CMTRIN (L7,CX,L7,DETERM)
C
      WRITE (6,2300)
 2300 FORMAT ('1','  ')
C
C     CALCULATE THE VALUE OF THE SAMPLE VECTOR
C
      WRITE (6,2350)
 2350 FORMAT ('0','THE SAMPLE VECTOR AT EACH SURFACE DIPOLE IS')
      DO 2400 M=1,L7
      X(M)=( 0.0, 0.0)
      DO 2500 N=1,L7
      R(N)=CX(M,N)*A(N)
      X(M)=X(M)+R(N)
 2500 CONTINUE
      WRITE (6,2600)M,X(M)
 2600 FORMAT (' ','X(',I3,')=',2X,E14.7,2X,E14.7)
 2400 CONTINUE
      WRITE (6,2700)
 2700 FORMAT ('1','    ')
C
C     CALCULATE THE VALUE OF THE SURFACE CURRENT (JS), ITS ABSOLUTE
C     VALUE (JSAB) AND ITS PHASE (JSPH)
C
      DO 3000 M=1,L7
      JS(M)=X(M)*(120.*PI)/(W**2)
      JSAB(M)=CABS(JS(M))
      JSRE(M)=REAL(JS(M))
      JSIM(M)=AIMAG(JS(M))
      JSPH(M)=(ATAN(JSIM(M)/JSRE(M)))*360/(2*PI)
      IF(JSPH(M).LT.0.0)JSPH(M)=JSPH(M)+360.
 3000 CONTINUE
      END
```

```
      COMPUTER PROGRAM 5
C
CC
CC    W=WIDTH OF DIPOLE (AND MONOPOLE)
CC    D=LENGTH OF MONOPOLE (HALF OF THE LENGTH OF DIPOLE)
CC    NPOINT=TOTAL NUMBER OF POINTS USED TO DESCRIBE THE SURFACE
CC    NSUR=NUMBER OF SURFACES (MONOPOLES) DEFINING THE SURFACE
CC    XLAMDA=WAVELENGTH IN METERS
CC    L1=NUMBER OF POINTS IN A ROW
CC    L2=L1-1
CC    L3=NUMBER OF ROWS OF POINTS
CC    L4=L3-1
CC    L5=L1*(L3-1)-L2
CC    L6=L2-1
CC    L7=NUMBER OF PATCHES IN A Z-DIRECTED PATH
CC    L8=NUMBER OF PATCHES IN A Y-DIRECTED PATH
CCC
      SUBROUTINE DATAIN(X,Y,Z,IS,ICP,NCP,NPOINT,PHI,THETA,POLAR,NSUR
     1                 ,NPATH,XLAMDA,NDIM1,NDIM2,NDIM3)
      DIMENSION X(1),Y(1),Z(1),IS(NDIM1,4),ICP(NDIM2,NDIM3),NCP(1)
C
CCC
CCCC  TITLE   RECTANGULAR PLATE
CCCC
CCC   INITIALIZATION
      W=1./8.
      D=1./8.
      NPOINT=45
      XLAMDA=1.0
      PHI=0.0
      THETA=90.0
      POLAR=90.0
      L1=9
      L2=8
      L3=5
      L4=L3-1
      L5=(L1*L4)-L2
      L6=L2-1
      L7=4
      L8=8
C
CCC
CCC   DEFINE COORDINATES OF POINTS
C
      DO 1 M=1,NPOINT
      X(M)=0.0
```

```
    1 CONTINUE
      Y(1)=-0.5
      DO 2 M=1,L2
      MPL1=M+1
      Y(MPL1)=Y(M)+W
    2 CONTINUE
      DO 3 M=1,L4
      INC=1+(M-1)*L1
      INCL2=INC+L2
      DO 4 N=INC,INCL2
      NPLL1=N+L1
      Y(NPLL1)=Y(N)
    4 CONTINUE
    3 CONTINUE
      Z(1)=-0.25
      DO 5 M=1,L5,L1
      MPLL1=M+L1
      Z(MPLL1)=Z(M)+D
    5 CONTINUE
      DO 6 M=1,L3
      INC=1+(M-1)*L1
      INCL6=INC+L6
      DO 7 N=INC,INCL6
      NPL1=N+1
      Z(NPL1)=Z(N)
    7 CONTINUE
    6 CONTINUE
C
C
C     DEFINE SURFACES
C
      NSUR=32
      IS(1,1)=1
      IS(1,2)=2
      IS(1,3)=11
      IS(1,4)=10
C
      MM=1
      DO 8 M=2,NSUR
      MM=MM+1
      DO 9 N=1,4
      IS(M,N)=IS(1,N)+(MM-1)
    9 CONTINUE
      DO 10 ICH=1,L4
      IFLAG=L2+(ICH-1)*L1
      IF(MM.EQ.IFLAG)MM=MM+1
   10 CONTINUE
    8 CONTINUE
```

```
C
C
C       DEFINE CURRENT PATH
C       WHEN CURRENT IN ONLY Z-DIRECTION (IPATH=1)
C       WHEN CURRENT IN Z-DIRECTION AND Y-DIRECTION (IPATH=2)
C
        IPATH=2
        NPATH=8+4
C
C       NCP(I)=TOTAL NUMBER OF SURFACES IN THE I-TH CURRENT PATH
C
        DO 11 I=1,L2
        NCP(I)=L7
   11   CONTINUE
        DO 21 I=1,L4
        JPATH=1+(I-1)*L2
        ICP(1,I)=JPATH
   21   CONTINUE
        DO 12 M=2,L2
        DO 13 N=1,L7
        ICP(M,N)=ICP(1,N)+(M-1)
   13   CONTINUE
   12   CONTINUE
C       CHECK IF THERE IS CURRENT IN Y-DIRECTION
        IF(IPATH.EQ.1)GO TO 20
        DO 14 I=L1,NPATH
        NCP(I)=L8
   14   CONTINUE
        DO 15 I=L1,NPATH
        IDUM=(I-L1)*L2
        DO 16 J=1,L8
        ICP(I,J)=J+IDUM
   16   CONTINUE
   15   CONTINUE
   20   CONTINUE
        RETURN
        END
```

BIBLIOGRAPHY

1. IIT Research Institute, "DNA EMP Awareness Course Notes," pp. 1-4, September 1971.

2. Burton, R. W., "The Crossed-Dipole Structure of Aircraft in an Electromagnetic Pulse Environment," Conference on Electromagnetic Noise Interference and Compatibility, North Atlantic Treaty Organization, Paris, October 1974.

3. Richmond, J. H. and Wang, N., Sinusoidal Reaction Formulation for Radiation and Scattering from Conducting Surfaces, NASA, CR-2398, June 1974.

4. Rahmat-Samii, Y. and Mittra, R., "Integral Equation Solution and RCS Computation of a Thin Rectangular Plate," IEEE Transactions on Antenna and Propagation, Vol. AP-22, No. 4, July 1974, pp. 608-610.

5. Butler, C. M., "Outlines of the Moment Method," Supplementary Notes for Wire Antennas and Scatterers, A Short Course in Electromagnetic Theory presented at the University of Mississippi, April 1972.

6. Harrington, R. F., "Matrix Methods for Field Problems," Proceedings of the IEEE, Vol. 55, pp. 136-149.

7. Bryant, M. L., An Application of the Piecewise-Sinusoidal Reaction Matching Techniques to Linear Dipole Antennas, MS Thesis, Naval Postgraduate School, Monterey, California, June 1973.

8. Rumsey, V. H., "Reaction Concept in Electromagnetic Theory," Physical Review, Vol. 94, June 1954, pp. 1483-1491.

9. Cohen, M. H., "Application of the Reaction Concept to Scattering Problems," IEEE Trans., Vol. AP-3, October 1955, pp. 193-199.

10. Harrington, R. F., Time-Harmonic Electromagnetics Fields, McGraw-Hill, New York, 1961, pp. 340-345.

11. Richmond, J. H., "A Reaction Theorem and its Application to Antenna Impedance Calculation," IEEE Trans., Vol. AP-9, November 1961, pp. 515-520.

INITIAL DISTRIBUTION LIST

		No. Copies
1.	Defense Documentation Center Cameron Station Alexandria, Virginia 22314	2
2.	Library, Code 0212 Naval Postgraduate School Monterey, California 93940	2
3.	Department Chairman, Code 52 Department of Electrical Engineering Naval Postgraduate School Monterey, California 93940	2
4.	Asst Professor Richard W. Adler, Code 52Ab Department of Electrical Engineering Naval Postgraduate School Monterey, California 93940	2
5.	Dr. J. H. Richmond Electroscience Lab. Ohio State University 1320 Kinnear Road Columbus, Ohio 43212	1
6.	Dr. Raj Mittra Department of Electrical Engineering University of Illinois Urbana, Illinois 61801	1
7.	Dr. C. M. Butler Department of Electrical Engineering University of Mississippi University, Mississippi 38677	1
8.	Mr. Al Mink, Code 6179 Naval Ships Engineering Center Hyattsville, Maryland 20784	1
9.	Mr. Tony Testa, Code 6174 Naval Ships Engineering Center Hyattsville, Maryland 20784	1
10.	Dr. S. Siahatgar, Code 6174 Naval Ships Engineering Center Hyattsville, Maryland 20784	1

11. Ms. Fran Prout, Code 6174 — 1
Naval Ships Engineering Center
Hyattsville, Maryland 20784

12. LTCOL Albert Cupka — 1
Chief ELA Branch
AFWL
Kirtland Air Force Base, New Mexico 87117

13. Mr. J. C. P. McEachen — 1
Naval Sea Systems Command
Code SEA OGT
Washington, D. C. 20360

14. LT R. B. Birchfield — 1
Naval Materiel Command
Code MAT 034
Washington, D. C. 20360

15. Dr. R. C. Hansen — 1
17100 Ventura Blvd., Suite 213
Encino, California 91316

16. Dr. Don Dudley — 1
Electrical Engineering Department
University of Arizona
Tuscon, Arizona 87521

17. Dr. A. Sankar — 1
MS R-1 1144
TRW Systems
1 Space Park
Redondo Beach, California 90278

18. CDR E. G. Neely, III — 1
Naval Electronic Systems Command
Code ELEX 094
Washington, D. C. 20360

19. Dr. R. Tanner — 1
Technology for Communications International
1625 Stierlin Road
Mountain View, California 94043

20. Dr. Fred Tesche — 1
Science Applications, Inc.
P. O. Box 277
Berkeley, California 94701

21. Mr. Walter Curtis — 1
Boeing Aerospace Co.
P. O. Box 3999
Seattle, Washington 98124

22. CDR Russ Shields — 1
Naval Electronic Systems Command
Code PME-107
Washington, D. C. 20360

23. Dr. B. Strait — 1
Electrical Engineering Department
111 Link Hall
Syracuse University
Syracuse, New York 13210

24. Dr. Art Sindoris — 1
USAECOM
Ft. Monmouth, New 07703

25. Mr. Phillip Blacksmith, Code LZR — 1
Air Force Research Lab,
L G Hanscom Field
Bedford, Massachusetts 01730

26. CDR USACEEIA — 1
Attn: ACCC-CED-RP
Ft. Huachuca, Arizona 85613

27. Mr. Russell M. Brown, Code 5252 — 1
Naval Research Laboratory
Washington, D. C. 20390

28. Mr. Dennis E. Fessenden, Code SA32 — 1
U.S. Naval Underwater System Center
New Longdon, Connecticut 06320

29. Mr. Joseph Halberstein, Code FVN — 1
Naval Weapons Laboratory
Dahlgren, Virginia 22448

30. MAJ Anthony Martinez — 1
AFCRL
Hanscom Field, Massachusetts 01730

31. Dr. E. K. Miller — 1
Lawrence Liv Lab
P. O. Box 808
Livermore, California 94550

32. Mr. John Potenza — 1
Rome Air Development Center
Griffiss, Air Force Base, New York 13441

33. Dr. John W. Rockaway — 1
Naval Electronics Laboratory Center
Code 2120
San Diego, California 92152

34. Mr. Carlyle J. Sletten, Code LZ/AF 1
AF Cambridge Research Laboratory
Bedford, Massachusetts 91730

35. LT Jose A. Rospigliosi Balta 1
Direccion de Instruccion
Minsterio de Marina
San Isidro
Lima, Peru

36. Director de Instruccion 1
Ministerio de Marina
San Isidro
Lima, Peru

Thesis 157247
R772 Rospigliosi Balta
c.1 Induced currents on
two dimensional elec-
tromagnetic planar
structures.